Journal of Controlled Release 366 (2024) 312–327

Contents lists available at ScienceDirect

Journal of Controlled Release

journal homepage: www.elsevier.com/locate/jconrel

Review article

Focused ion beam-scanning electron microscopy provides novel insights of drug delivery phenomena

Thilo Faber [a], Jason T. McConville [b], Alf Lamprecht [a,c,*]

[a] Department of Pharmaceutics, Institute of Pharmacy, University of Bonn, Bonn, Germany
[b] Department of Pharmaceutical Sciences, College of Pharmacy, University of New Mexico, Albuquerque, NM, USA
[c] Université de Franche-Comté, INSERM UMR1098 Right, Besançon, France

ARTICLE INFO

Keywords:
Scanning electron microscopy
Imaging
Intracellular delivery

ABSTRACT

Scanning electron microscopy (SEM) has long been a standard tool for morphological analyses, providing sub micrometer resolution of pharmaceutical formulations. However, analysis of internal morphologies of such formulations can often be biased due to the introduction of artifacts that originate from sample preparation. A recent advancement in SEM, is the focused ion beam scanning electron microscopy (FIB-SEM). This technique uses a focused ion beam (FIB) to remove material with nanometer precision, to provide virtually sample-independent access to sub-surface structures. The FIB can be combined with SEM imaging capabilities within the same instrumentation. As a powerful analytical tool, electron microscopy and FIB-milling are performed sequentially to produce high-resolution 3D models of structural peculiarities of diverse drug delivery systems or their behavior in a biological environment, i.e. intracellular or -tissue distribution. This review paper briefly describes the technical background of the method, outlines a wide array of potential uses within the drug delivery field, and focuses on intracellular transport where high-resolution images are an essential tool for mechanistical insights.

1. Introduction

As highlighted by two Nobel prize recipients in recent years [1,2], improvements in microscopy have the potential to invigorate many research areas [3,4]. Drug delivery research utilizes a large variety of microscopy techniques, due to sample heterogeneity and the broad range of magnifications used in the field [5]. Various light microscopy techniques, such as polarized light microscopy and confocal laser scanning microscopy (CLSM) are routinely used in drug delivery research. Additionally, electron microscopy (EM) based techniques are frequently used, especially when resolutions below the diffraction limit of light are required [6,7]. Many small structures of interest, especially in the field of nanomedicine, are below the limit of light microscopical techniques since the size of the particles used in nanomedicine is often smaller than this diffraction limit of light [8,9]. As a consequence, such small particles can only be resolved as blurred spots in a given field of view [6,10,11]. Furthermore, another issue is that many nanoparticle imaging techniques rely on the use of contrast agents or dyes which can potentially leach from the particles of interest [12], potentially confounding the localization of nanomedicines [13–15]. Thus, EM is a commonly used imaging tool for the characterization of drug carriers [5,16]. Although transmission electron microscopy (TEM) surpasses scanning electron microscopy (SEM) in terms of resolution, however TEM has narrower sample stipulations and has especially cumbersome sample preparation requirements. For example, TEM requires ultra-thin samples for analysis, often below 100 nm [17]. As such, larger or bulky samples need to be sectioned using an ultramicrotome. Typical samples are ultra-thin sections of polymers [18–20], embedded biological samples [21,22] or samples in the nano-sized range, such as dried suspensions of nanoparticles [23–25] or viruses [26], both of which can be dispersed on to TEM grids prior to imaging. When considering pharmaceutical dosage forms for TEM imaging, only a limited number of samples meet these requirements or can undergo suitable sample preparation without the formation of image artifacts. The use of SEM is more common, due to its ease of use and broad applicability to a wide variety of sample types. However, despite these advantages SEM depicts only surfaces or subsurface features, making its suitability dependent upon appropriate sample selection and preparation. The appropriate sample preparation is essential for the successful imaging of sample features like internal structures of a drug delivery system, such as pores

* Corresponding author at: Department of Pharmaceutics, Institute of Pharmacy, Gerhard-Domagk-Straße 3, 53121 Bonn, Germany.
E-mail address: alf.lamprecht@uni-bonn.de (A. Lamprecht).

https://doi.org/10.1016/j.jconrel.2023.12.048
Received 15 November 2023; Received in revised form 23 December 2023; Accepted 26 December 2023
Available online 5 January 2024

[27,28] or drug-excipient distributions [29–31]. Such internal structures are either created purposely as a part of formulation strategy, or are introduced unintentionally during their production. For such small internal structures, there is a greater challenge in obtaining a suitable image, especially with advanced delivery systems such as micro- or nanoscale systems [32–34]. For example, in the case of polymeric nanocapsules, the microstructure is of crucial importance for the proposed delivery mechanism [33,35].

Only when structural properties are resolved, a direct relationship between structure and function can be established; and assumptions can be made about how a drug delivery vehicle might fulfill its delivery purpose, e.g., delivery across biological barriers [36]. Since, some internal features of drug formulations are too small to be analyzed by light microscopy and there are drawbacks of using TEM, sufficient resolution can be achieved with sample cross-section analysis using SEM. Standard approaches for the preparation of sample cross-sections are grinding, cutting, or (cryo)-fracturing procedures. However, each of these preparation methods present a risk of artifact generation. Such artifacts commonly include the obscuration of cross-sectional features due to smearing of sample material, the deposition of fragments, or the creation of uneven surfaces [27,37–41], as indicated (Fig. 1 A,B). The stability, size, and physical state such as, brittleness or elasticity of many pharmaceutical samples can present challenges in sample cross-sectional preparation [32]. For example, polymers represent a commonly used class of pharmaceutical excipients that should be cut by ultramicrotomy below their glass transition temperature due to their rubber-like nature [42], or at cryogenic temperatures to avoid smearing/dragging artifacts caused be compression forces associated with the use of a microtome blade [20]. This represents a major hurdle in sample preparation, as most polymeric systems contain glass transition temperature-lowering components such as, an active pharmaceutical ingredient (API), residual moisture, or other plasticizing agents [43,44]. Depending on size or stability, some drug delivery vehicles may need to be embedded prior to ultramicrotomy or fracturing, with the risk of artifacts being caused by the embedding medium or solvents used during preparation. Other commonly used excipients are not solid at standard operating temperatures (i.e. room temperature), and therefore require the maintenance of cryogenic conditions throughout the preparation or even the analysis [24,45,46]. As a consequence artifact free preparation of cross-sections is challenging, if it is possible at all [42,47]. Most of the aforementioned preparation methods have the additional disadvantage of not being site-specific, as it is difficult to precisely create the cross-section at the desired location. Additionally, most of these techniques require experience, so results can vary greatly due to the operator or analysis facility, since everyone performs these tasks differently. Thus, the ability to generate clean cross-sections without artifacts is of great interest in pharmaceutics, and is a fundamental requirement for precise analytics using SEM.

The use of a focused ion beam (FIB) is an alternative technique for producing site-specific cross sections. FIB accurately removes sample materials precisely at the desired location due to acceleration of high atomic mass ions focused at a given sample substrate surface. This process is referred to as FIB milling with material removal caused by ion impact, FIB-milling is considered a sputtering process [48–51]. Material removal by lasers is based on ablation, and is therefore based on different physical process. The amount of sample removal is highly dependent on the type of ions used, with gallium, argon, or xenon ions being the most common sources. These ions can also be used for

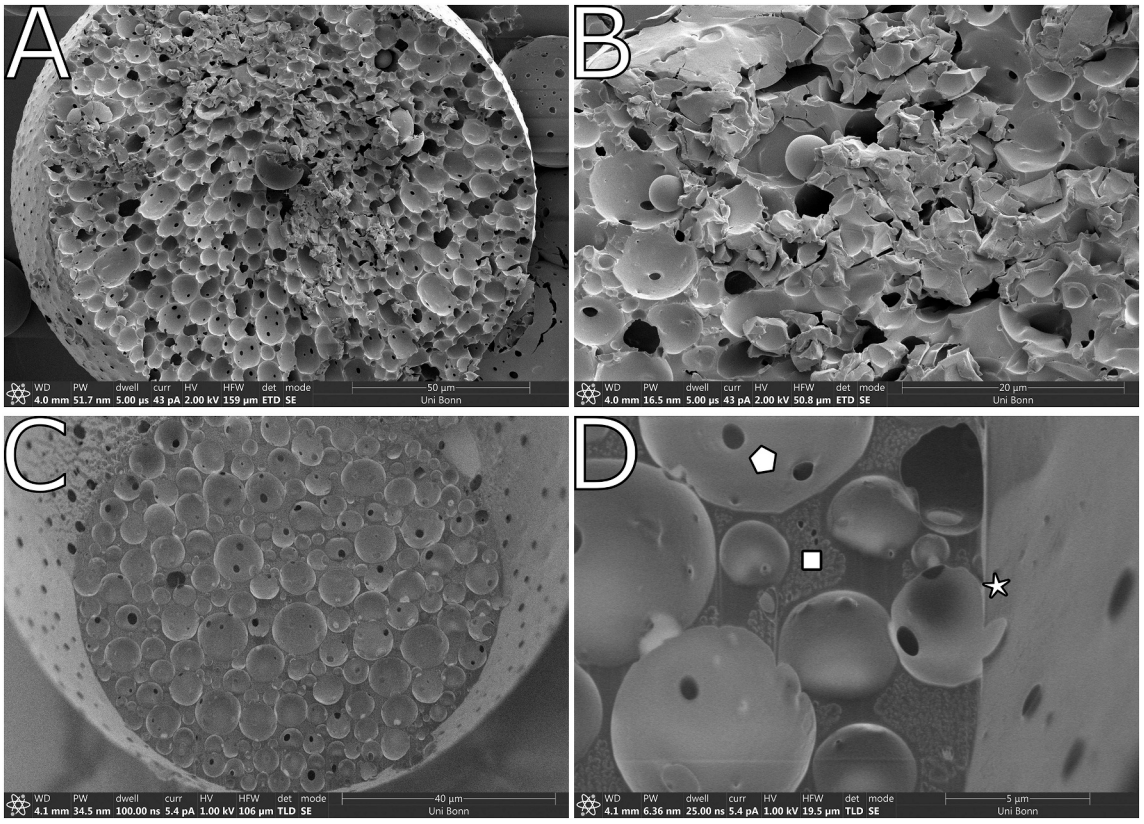

Fig. 1. Comparison of classical fracturing (A,B) with a FIB prepared cross-section (C—D) of double emulsion prepared poly(lactic-*co*-glycolic acid) (PLGA) microparticles (water in oil in water). (A) An overview of the particle's fracture edge. (B) An uneven surface with sample preparation artifacts caused by sample debris, hiding void structures or making them difficult to analyze. (C) FIB-SEM image where the cross-section through a particle was prepared using FIB-milling, then imaged using the integrated SEM. No artifacts are visible on the cross-section of the particle. (D) Higher SEM magnification of the FIB-milled sample demonstrating the high resolution afforded with no artifact interference. It shows an internal cavity with interconnecting pores (polygon), nanosized closed pores between the larger cavities (square), and a thin polymer membrane with a pore spanning across a void with no apparent distortion in membrane or pore shape (star).

imaging, but due to their destructive nature, material removal or manipulation is usually their main purpose. If the main purpose is imaging, helium ions are regularly used, e.g., in a helium ion microscope [52,53]. Alternatively, FIB can be combined with an electron microscope to create a focused ion beam scanning electron microscope (FIB-SEM). The standard configuration of a FIB-SEM consists of a gallium liquid metal ion source (LMIS) [54], and an electron source combined in a single microscope. This combination unites high resolution electron microscopy and FIB-milling in the same device [55], which will be described later in detail. When using FIB for material manipulation, as with any preparation technique, the process must be optimized for each sample depending on its specific composition, since ion milling is a destructive high-energy process. If the milling settings are adjusted accordingly [56], clean and flat cross sections can be prepared almost independent of the material, whilst still preserving complex microstructures (Fig. 1 C,D).

One of the first uses of FIB-SEM in pharmaceutical sciences was in 2006 to image the internal structure of microspheres prepared by a conventional double emulsion technique [57]. Since then, the technique has been applied to other areas of drug delivery such as, the analysis of coatings, microparticles, implants, and tablets. It is most commonly used for detailed examination of micro/nanopores to determine spatial location and dimensions in certain drug delivery systems (DDS) [58,59]. The true potential of FIB-SEM is not solely the ability to ablate most materials at the exact point of interest, but to perform FIB-SEM tomography using FIB-milling and SEM imaging in an alternating manor to transpose 2D images into 3D volume analysis for model reconstructions. This tomography technique can be used to generate 2D image stacks with a known slice thickness that can be aligned, segmented, and finally combined and reconstructed in an 3D image. This type of precise structural investigation has demonstrated great importance in structural biology, with its ability to generate high resolution 3D models of tissues and cells [60,61]. This approach is equally applicable in drug delivery, for example to enable the investigation of cellular nanoparticle uptake and determination of their intracellular fate in 3Dor study the drug carrier itself [29], thereby demonstrating a wide range of possible applications within the field of pharmaceutical technology and drug delivery.

This review aims to introduce recently reported additional visualization options using FIB-SEM imaging approaches across the field of drug delivery. We present research with a fundamental technical background of the method, to enable the reader to assess the potential applicability of FIB-SEM in their own research. Additionally, this review will give an overview for applications of FIB-SEM in areas of advanced drug delivery, especially in the context of intracellular trafficking of nanosized drug delivery systems.

2. FIB-SEM sample preparation and workflow

In general, sample preparation methods for FIB-SEM are comparable to standard SEM techniques, for example affixing a formulation to a sample stub then sputter coating it using a carbon, gold, or platinum target to make the sample surface conducting. Biological samples are typically fixed and stained using TEM staining and embedding protocols. Such samples must be dehydrated with organic solvents such as ethanol or acetone before embedding in a resin to allow thin sectioning with (ultra)microtomy. In the case of FIB-SEM biological sample preparation is similar, but further optimization may be needed, for example with successive osmification steps due to weaker signal strength, compared to TEM. In addition, FIB SEM samples are larger because they are analyzed as bulky samples rather than ultra-thin sections, making them more susceptible to charging. [62–64].

2.1. Special aspects of FIB-SEM investigations

For FIB-SEM investigations, the microscope is operated much like a standard SEM. When a region of interest (ROI) is found, a sample is positioned at the eucentric point (the sample stage position where the electron beam and the ion beam focus on the same point). For this purpose, the sample stage is oriented at a precise angle, dependent on the microscope manufacturer specification (e.g., 52° could be the standard sample tilt for Dualbeam™ FIB-SEMs (Thermo Fisher, Eindhoven, Netherlands [former FEI-Company])) or dependent on the sample pretilt. Depending on the durability of the sample to the ion beam, a protective platinum pad may be applied. Such a pad is prepared by FIB-assisted chemical vapor deposition of an organo-platinum compound (e.g trimethyl–methylcyclopentadienyl–platinum) which is volatilized using heat and the high vacuum conditions of the microscope chamber, it is released by a gas injection system near the ROI. The organic framework of the organo-platinum compound is decomposed by the ion beam resulting in local platinum deposition [65] in a selected area. The platinum deposition is especially important when performing FIB-SEM tomography, since the tomography application acquires several hundred or thousand images with the ion beam from the same region. As every ion beam image damages the surface within its field of view, the ROI is thus protected from the unintentional beam damage (Fig. 3). As outlined below, there are two possible procedures to prepare a sample for imaging, depending on the sample size and morphology.

2.1.1. Small or particulate samples

If the sample is free standing and directly visible (Fig. 2 A), it can be directly milled. This type of sample is easily accessible when using FIB-SEM (Fig. 2B), because the structures of interest are visible and not obscured by embedding resin or the sample material itself (Fig. 2C); which could be the case when probing a region within a bulky sample such as a tablet. This direct accessibility is often the case for particulate samples of a suitable size range, or for biological samples prepared using a minimal resin embedding procedure [66,67]. If the goal is to prepare a cross-section for qualitative analysis, larger samples of about 100 μm may still be acceptable. However, for volume analysis by acquiring a 2D image stack, much smaller sample sizes are preferable since the processing time required increases considerably.

2.1.2. Large or bulky samples

Large samples like tablets, implants, resin embedded cells or tissues (Fig. 3 A) need additional preparation steps. These samples typically require the construction of front and side trenches (Fig. 3B) to aid in the visualization of internal structures of interest (Fig. 3C). In particular, a front trench is important because it allows the electron beam to access the sample cross section. Trench development ensures that sufficient and unhindered electron signals can be collected directly from the prepared cross-section. Additionally, trenches ensure that milled material is cleanly removed at the cross-section surface, which is especially important when performing FIB-SEM tomography. The preparation of cross sections, especially for FIB-SEM tomography, in a bulky sample is inherently more time consuming due to the need for trenching in a larger sample.

2.1.3. FIB-SEM lift-outs

The available SEM resolution might be not sufficient for every sample situation, since the imaging of the cross-section using FIB-SEM is still reliant and limited to the inherent resolving power of the SEM used. The FIB-SEM technique also permits side-specific sample preparation of thin lamellas for TEM investigations. To achieve this, a thin piece of the sample can be cut out using the FIB and then lifted out using a micromanipulator, a dedicated device installed in a FIB-SEM microscope that allows high precision sample maneuvering within the microscope chamber. The lamella can then either be transferred to a sample preparation grid, and then be investigated using a standalone TEM, or directly measured if the FIB-SEM is equipped with a transmission detector. Such sample lift-outs can enable advanced analytical techniques like electron diffraction, for crystal structure analysis. [55,57,68–70].

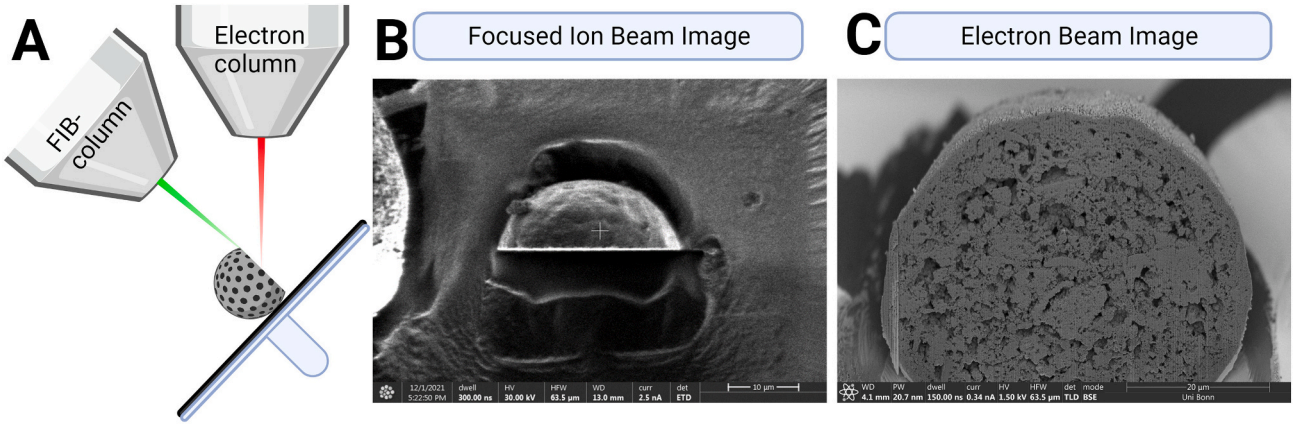

Fig. 2. Schematic overview (Fig. 2A) of an FIB-SEM prepared free standing particle for acquisition of a 2D image stack. Showing the FIB perpendicular to the particle so that it can image and mill the particle from top view (Fig. 2B). The electron beam images the revealed cross sections through the particle in tilted state (Fig. 2C).

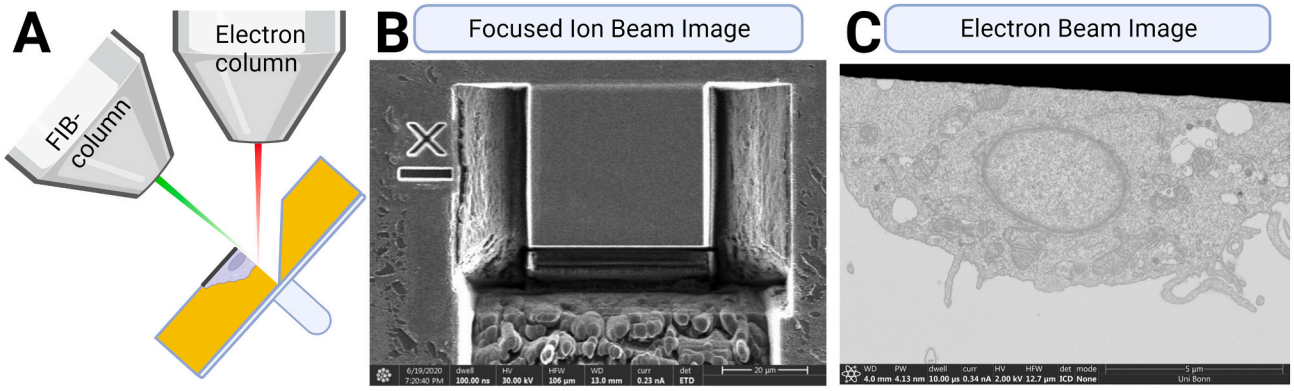

Fig. 3. Schematic overview (Fig. 3A) of an embedded cell culture sample prepared with the FIB-SEM, showing all the preparatory steps required to acquire a 2D image stack. The schematic shows the sample in a tilted state, perpendicular to the FIB and already protected with a platinum pad and the necessary trenches to give the electron beam access to the cross-section. The FIB image (Fig. 3B) shows a typical fully prepared sample prior to acquisition of the 2D image stack, with the platinum-protected square shaped VOI in the center of the image and the front and side trenches surrounding it. On the left side of the FIB image is a typical fiducial mark in the form of an underlined X, which the automatic imaging software needs to recognize the position. The backscattered electron image (Fig. 3C) shows the embedded cell with inverted contrast to mimic the cell images normally obtained in TEM examinations. The dark area at the top of the image, where the cell appears to be growing on, is the electron-dense platinum protective layer.

Lamellae lift-outs at cryogenic temperatures can enable the investigation of vitrified or environmentally sensitive samples (e.g. thermally labile structures). The extensive capabilities of the lift-out technique have not been thoroughly investigated in the field of pharmaceutics, and to-date it has only be used for the investigation of PLA microparticles. In that study, the lift-outs were analyzed for crystallinity using electron diffraction and high resolution TEM imaging [57].

2.2. Limitations of the FIB-SEM technique and alternatives

Since many pharmaceutical samples contain liquid or semi-solid excipients, analysis may need to be conducted under cryogenic conditions. Cryo-electron microscopy requires even more specialized equipment, experienced operators, and complex sample preparation methods. The most significant limitation of a typical gallium LMIS-based FIB-SEM microscope in the field of drug delivery science, is the size of the cross sections that can be produced in a reasonable amount of time, since a 100 μm wide and 50 μm deep cross-section could easily take several hours. Therefore, the technique provides high resolution images but is only suitable to a limited imaging area in larger samples such as tablets, pellets, granules, capsules, or implants and these systems need to be fragmented before being examined locally.

In a case, where volume imaging is not essential but only high cross-sections are sought, broad ion beam (BIB) devices may be a suitable alternative, which are capable of processing larger samples with an unfocused broad beam of ions, usually argon. These systems are offered as stand-alone sample preparation devices and can be combined with any suitable microscope, such as a SEM [33,37]. As indicated, BIB milling systems are far from being a standard preparation technique in drug delivery [33,37], but are well established in other fields such as geology [71–75], dental research [76,77], or materials science [78–80]. To date, BIB milling has not been commercially available as a tomography tool for EM investigations [81], and is therefore limited to 2D cross sections.

2.3. Pitfalls and artifacts

Since any imaging and sample preparation technique carries the risk of generating artifacts, identifying such artifacts, and understanding their causes is critical for successful image interpretation and method development. This is also true for the FIB-SEM technique. Artifacts include those commonly associated with standard SEM imaging (Fig. 4D, F), such as charging [82], carbon contamination [83,84], shadowing [85], or electron beam damage [86]. Additionally, the focused ion beam itself can cause its own set of artifacts, since ion imaging and milling a sample is destructive process as can be seen in the

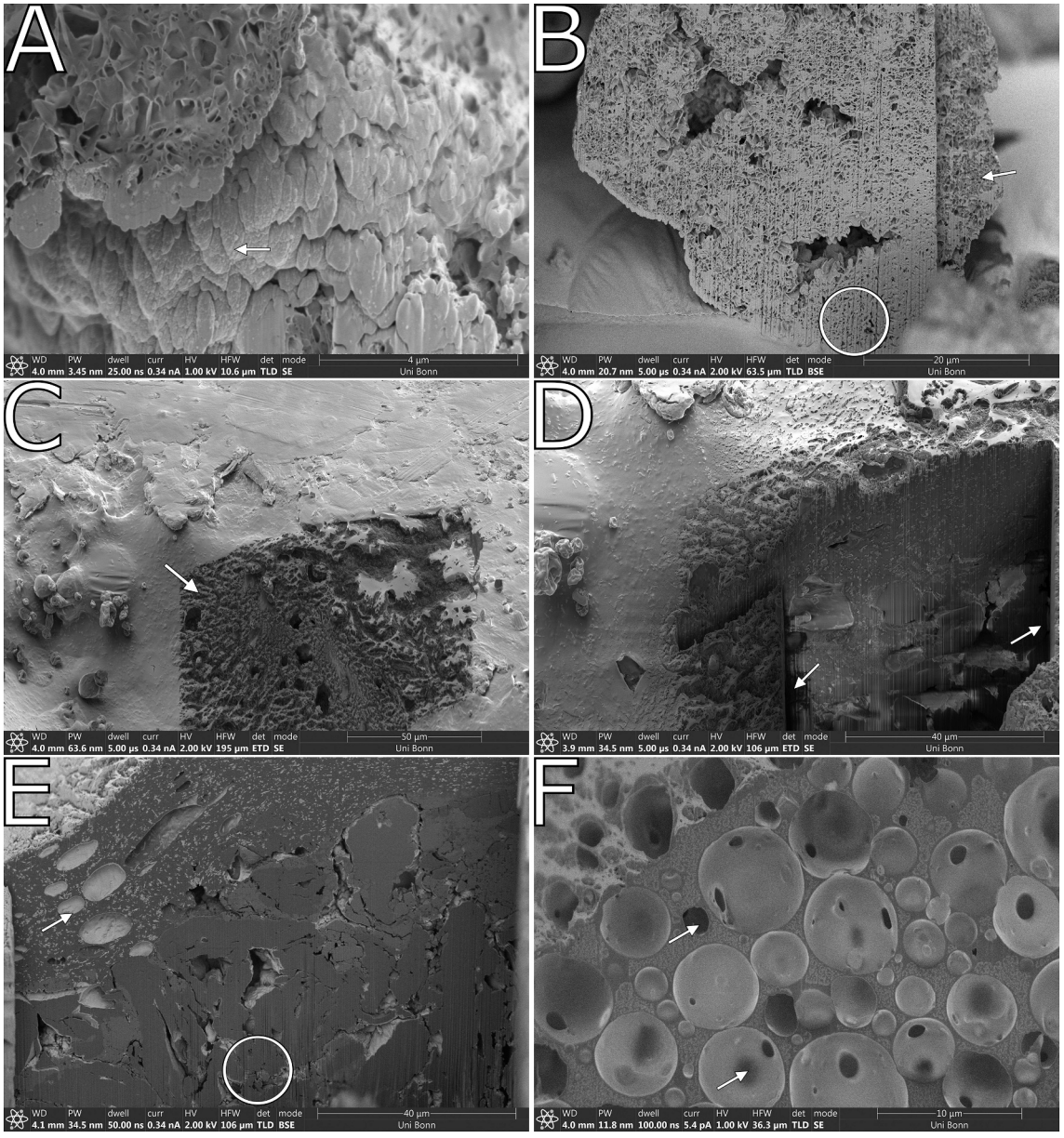

Fig. 4. Various imaging and preparation artifacts (unpublished data) from several DDS, with (A,B) being a porous silica sample, (C-E) a tablet and (F) a PLGA microparticle prepared by double emulsion technique. Figure section (A) shows a milled mesoporous silica sample with clearly visible porous platelet-like structure. At the lower edge and at the neighboring particle electron dense material redeposited during milling. The redeposition shows a characteristic drop shape structure with a grainy surface. Section (B) demonstrates severe curtaining after high current milling, which intensifies with milling depth. The right particle side was additionally fine polished with a lower current ion beam, reducing the curtaining immensely. On image section (C) the surface damage of a tablet caused by the Ion beam. Segment (D) shows the same region after milling an insufficient front trench, shadowing can be seen at both edges of the cross section, as well as at the bottom due to the insufficient length of the trench. Section (E) the final prepared cross-section of the tablet, in which all features are clearly visible, from the pigment-containing coating with voids containing bright redeposition artifacts to the excipient particles. The double emulsion microparticle (F) displays various electron imaging artifacts especially in the large intraparticular voids from bright and dark charging artifacts.

surface damage of a tablet after imaging (Fig. 4C). The most common are redeposition, curtaining, gallium ion implantation, and heat-related damage. Heat-related damage includes melting, amorphization, or degradation [85,87–90]. Additional artifacts involve embrittlement or phase changes due to ion irradiation [91,92], but these are not as relevant for pharmaceutical samples. Redeposition can occur on all surfaces in proximity the ion beam milling site [93,94]. Depending on the ion beam current applied, the redeposition may have the appearance of a pattern covering the surfaces and reducing image contrast, essentially making the image have a more grayish hue. Large-scale redepositions can appear as droplet-like structures formed by high-current FIB-milling [85] (Fig. 4A) on surfaces near the milling site, as seen on the adjacent porous silicate particle. Furthermore, in the presence of a porous matrix, accumulation within the pores is possible, manifesting as an electron-dense pattern that can be confused with encapsulated material [95] (Fig. 4E). Fig. 4E shows a commercial tablet with voids observed in the coating, some of which have dense electron deposition inside. To reduce redeposition, less material must be milled per unit time, so that the vacuum of the system is able to adequately remove the sputtered material. Curtaining, as the name suggests, has the appearance of a wavy curtain or cascading waterfall (Fig. 4 B, E encircled areas) which can be seen on the cross-section of the porous silica carrier (Fig. 4 B) and on the tablet bevor low current FIB-polishing manifesting as vertical stripes (Fig. 4D and E encircled areas). There are many possible causes for

curtaining, including uneven surfaces, a porous material, or composites of soft and hard material [96]. The ripples associated with curtaining influences the image quality of the cross section and can obscure small features, rendering cross-sections "noisy". The curtaining effect tends to be more prominent with increased milling depth. Heat damage can be minimized either by reducing the current and dwell time of the ion beam, or by working at cryogenic temperatures. Thermal influence can be difficult to detect and can have the appearance of an amorphous-looking surface with rounded rather than sharp edges, or structures appearing to be bent or deformed due to softening or melting [97–100]. Shadowing is a phenomenon which happens when the generated electron signal does not reach the detectors adequately, thus giving the appearance of darker regions (Fig. 4 D). Shadowing is caused by structures blocking the signal after insufficient trenching, and occurs especially near sample edges.

Current challenges in pharmaceutics when using EM techniques to characterize drug formulations is the low contrast between most pharmaceutical excipients and APIs, their non-conductive nature, and the overall complexity of drug formulations as well as their size and physical state. The low contrast differences can be partly compensated using EDS systems [29] or by the development of staining protocols, since they are often used with biological or polymeric samples for EM investigations.

3. Applications of FIB-SEM in drug delivery

To date the FIB-SEM technique has mostly been used for the morphological characterization of DDS, mainly focusing on internal structures of polymeric sustained release dosage forms, such as microspheres, implants, or the polymeric coatings of controlled release formulations. In addition, further studies have been conducted on spray-dried, mesoporous particles, and tablets. This section describes the various application fields of FIB-SEM within drug delivery.

3.1. Depot formulations

Long-acting microspheres are complex drug carrier particles with have a variety of internal features that cannot be adequately captured by SEM because many critical features are localized within the carrier itself; including pores and API crystals generally distributed throughout a polymer matrix. As several studies have shown, FIB-SEM is very useful in characterizing the internal structure of such microspheres. The first application of FIB-SEM was performed on polylactic acid (PLA) microspheres loaded with naltrexone, prepared using a double emulsion solvent evaporation method [57]. Here, microsphere particle surfaces were peeled off by scanning an ion beam over the surface. Although this method removes material from the surface, it did not provide the quality of images obtained when using the FIB as a tool for cross-sectioning, because the material was not removed homogeneously. This early approach for pore analysis of the carrier made it difficult to assess exact pore size and morphology, since this type of surface milling does not result in a clean sample cross-section. In such instances, deformation of the particle can be caused by the ion beam, obscuring morphological features, with the authors reporting that the first pores became visible after milling to a depth of about 4 μm. In addition to surface peeling, TEM lamellae were prepared at various locations on the sphere, lifted out and then transferred to a TEM. TEM examination of the lamellae revealed no observable atomic order and no distinct electron diffraction patterns, from which the authors concluded that the probed regions were amorphous.

Preparation of cross-sections for pore analysis has been established for micro- and nanoparticles made from various materials, including: chitosan [101], PLGA [29,32,102–104], PLGA-lipid mixtures [58], or mesoporous silica nanoparticles [105]. One research group used phase-contrast nano-computed tomography (CT) to compare pore size results from FIB-SEM studies for PLGA-lipid microspheres and confirmed the concordance of results between the two techniques [58]. Furthermore, owing to the high resolution of the FIB-SEM, it was possible to detect anisotropic material in the pores that was not clearly visible using the nano-CT data [58]. FIB-SEM has also been applied to study the degradation process of levofloxacin loaded PLGA microspheres over 5 days under drug release conditions. And, while the shift from spherical to collapsed particles was well known before, using standard SEM methodologies [106], FIB cross-sections could be used to elucidate the progress of the internal porosity change over a 5-day period [102] (Fig. 5). The pore size increases over this time significantly with a change in shape from round to corrugated particles. The major benefit of the FIB technique in this context, is the possibility to image internal structures that are not accessible with the same level of resolution with the use of alternative techniques such as CT. A comparable experiment on the morphological changes of the microspheres was performed before and after 5 days of drug release [29]. In this study, 3D structures were generated from microspheres before and after drug release and used for various calculations and numerical simulations. For example, the authors were able to determine the drug diffusivity from the resulting drug particle/pore networks within the matrix. It was also found that the embedded drug particles within the microsphere are dissolved from the outer to the inner layers.

In addition to 2D cross-sectioning, FIB-SEM tomography can enhance the depth of information from such investigations. For example, it is possible to use the 2D image stacks to render 3D models which can be analyzed for further information (Fig. 6). FIB-SEM tomography has garnered recent interest for studying implants or long-acting injectable microspheres composed of PLGA. After this stacking/segmentation of microsphere images, critical quality attributes (CQAs) can be better described by observing the 3D rendered datasets, rather than an isolated standard unprocessed 2D section. This approach to whole particle modelling allows the user to assess among other things, the amount of embedded drug particles and their size, the porosity of the particle matrix, as well as a quantitative assessment of the amount of polymer present. Especially, the porosity can be much better evaluated in a 3D model compared to the conventional 2D slices [32].

Comparable studies have been performed on hot melt extruded PLGA [30] or ethylene vinyl acetate (EVA) implants [31]. In these studies, a combination of X-ray microscopy or micro-CT and FIB-SEM was used to create 3D models for predicting drug release profiles of the formulations. The results of the X-ray microscopy-based models and drug release prediction agreed well with an observed initial burst release of the active, but was not suited to describe the entire dissolution profile. Image-based drug release prediction profiles using additional FIB-SEM data sets in the prediction model were able to predict drug release with up to 5% accuracy compared to measured release [30,31,104]. When the FIB-SEM data were neglected, the accuracy of the prediction was worse. As an alternative to X-ray microscopy, micro-computed tomography (micro-CT) can be used to image larger samples. Both techniques, FIB-SEM and X-ray-microscopy/micro-CT applied in a correlating imaging workflow could be used to analyze DDS, not only in terms of porosity and dispersed drug particle size, but also to create drug release prediction models. FIB-SEM provides the necessary resolution to analyze smaller features in carrier systems that are not visible from the surface, and cannot be detected by other volume imaging methods. In these studies, the observed microstructures proved essential in predicting drug release successfully. Since FIB-SEM is unable to characterize large sample volumes due to its slow processing speed, the combination of FIB-SEM with micro-CT or X-ray microscopy can be used to describe a drug carrier system in a way the prediction of its drug release may be possible. Such observations could be used to enhance the understanding of a drug release profile from microparticles, or other types of depot formulations.

3.2. Tablets and compacts

Tablets and compacts are well suited for analysis using other

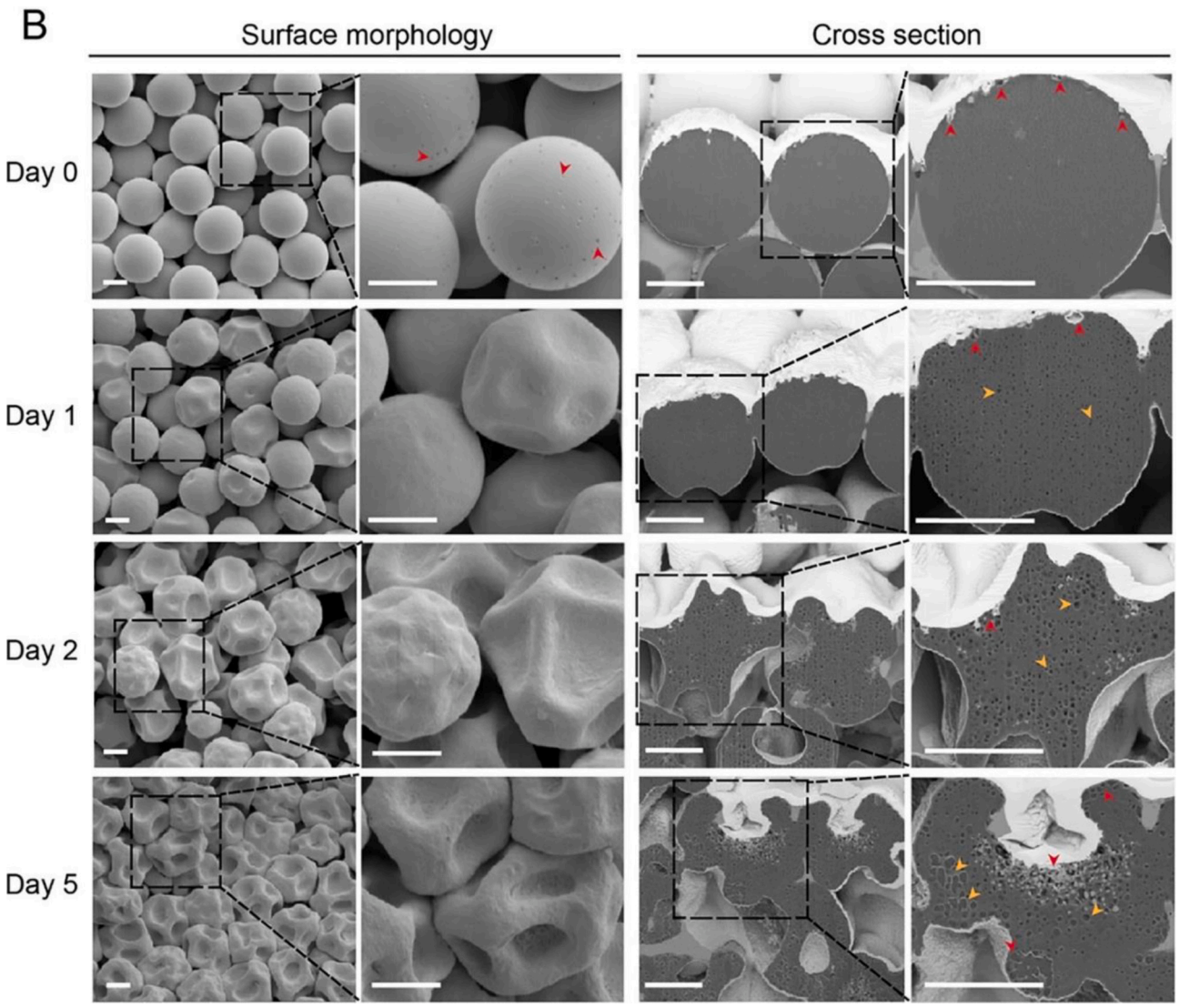

Fig. 5. Drug release and structural changes of PLGA microspheres over the duration of 5 days investigated by SEM for surface morphology and FIB-SEM for the cross sections. Arrows indicate Internal (orange) and external (red) pores. Reprinted and adapted with permission from [102]. Copyright {2020} American Chemical Society." (For interpretation of the references to colour in this figure legend, the reader is referred to the web version of this article.)

standard analysis methods (e.g. micro-CT, or MIP) as these methods are capable of acquiring data for the entire dosage form or at least a large area of it, allowing the user to investigate most of the internal structure. However, FIB-SEM can be used to complement mercury intrusion porosimetry datasets, as it is able to view detailed porous structures [107]. In addition, it is possible to probe different areas of a tablet to investigate for example, magnesium stearate deposits [108].

Micro-CT or X-ray microscopy could be used to analyze the formulation as a whole and enable to detect specific regions of interest that subsequently can be depicted at highest resolution using FIB-SEM. Due to the non-destructive nature of micro-CT or X-ray microscopy imaging, it is theoretically possible to analyze a tablet with micro-CT, label a region of interest in the resulting data set and reanalyze this region with high-resolution imaging technique such as FIB-SEM. The potential advantage of the use of a combination of micro-CT and the FIB-SEM technique for larger samples is the ability to obtain a quick overview and further analyze particle interactions or nanostructures more precisely.

3.3. Pharmaceutical coatings

Coatings are widely used in the pharmaceutical industry, and range from aesthetic finishes to sophisticated controlled release encapsulations. As referenced earlier, the applicability of FIB-SEM for the analysis of microstructural features of microspheres also suggests that its use is suitable for the study of coatings for pharmaceutical applications. For the example with controlled release coatings, drug release can be influenced by the addition of pore-forming agents that form microstructural porous networks during dissolution as the agent leaches from the applied coating [109–112]. For this reason, the study of these porous coatings is of interest and has already been investigated using SEM on either freeze-fractured films, microtome sections, or directly on coating surfaces [111,112]. Such studies have provided high quality visualization of pores, but have ultimately concluded that the analysis of pore shape, size and connectivity could be more accurately described if performed using a 3D structure. This type of analysis would further improve the understanding of the specific mechanism of drug release from porous systems in controlled DDS. Investigations with this aim were conducted recently using isolated pre-leached ethylcellulose (EC) films, which could be considered a challenging but typical model for electron

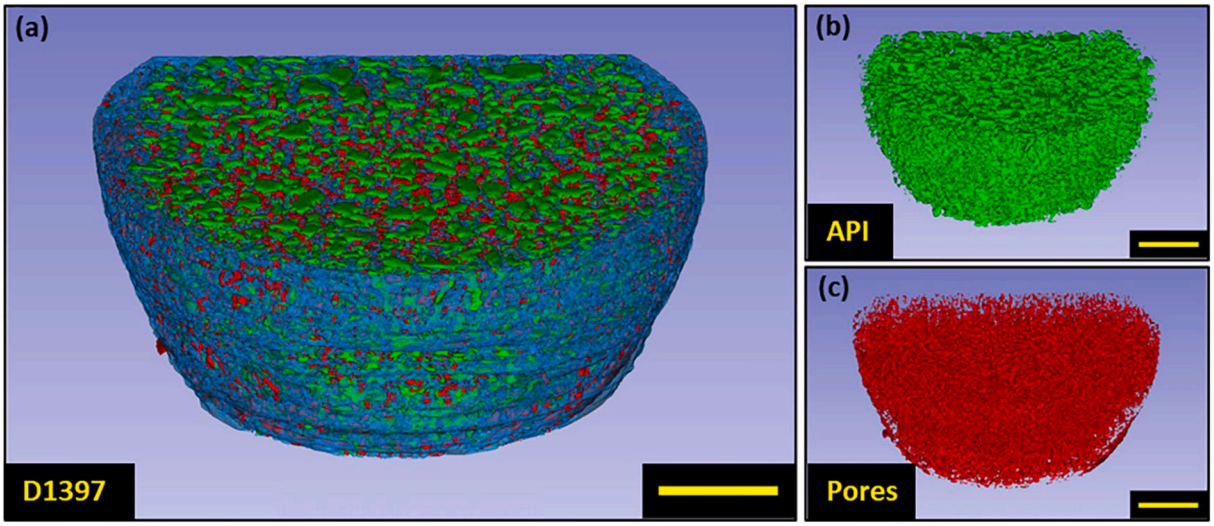

Fig. 6. Digitally reconstructed polymeric microsphere from FIB-SEM 3D reconstruction, with (b) showing the drug crystals in green and (c) showing the isolated pore phase in red, combined with the polymer phase colored in teal (a). Reprinted from [32] with permission from Elsevier. Copyright (2021) Journal of Controlled Release. (For interpretation of the references to colour in this figure legend, the reader is referred to the web version of this article.)

microscopy within pharmaceutics [85]. Pre-leached EC films were prepared using EC as a water-insoluble extended-release polymer and hydroxypropyl cellulose (HPC) as a water-soluble pore-forming polymer with three different HPC weight percentages, i.e. 22%, 30%, and 45%, in the dried film. The films were prepared by coating a rotating drum according to a previously described method [113]. These investigations describe the various steps of FIB-SEM from imaging and image stack alignment and segmentation [114], to the reconstruction and 3D modelling (Fig. 7) [115].Reconstructed 3D models were analyzed in terms of pore size and connectivity [116,117], as well as for simulations of mass transfer through the ethyl cellulose film, after permeability was measured experimentally with tritiated water in a two chamber diffusion cell [118].

In addition to the analysis of isolated polymer films described above, it is also possible to perform such studies on a finished drug delivery system, such as controlled release drug coated pellets The analysis of the finished pharmaceutical product allows investigations to be performed, both before and after drug release has occurred [119]. In a previous study, investigators were able to successfully observe the microstructural changes of a coating before and after drug release, while simultaneously quantifying coating thickness in the sample. In addition, models created using FIB-SEM tomography can better represent the pores and their distribution within a matrix system in greater detail than conventional SEM, allowing the user to analyze of the tortuosity of a pore network in a given sample coating. For example, a 2D surface or layer image is not able to resolve the complex nature of the pore networks in a controlled release coating or other porous matrix, because interconnecting pores from deeper layers are not accessible or they may be too small for other volume imaging techniques. FIB-SEM can improve the understanding of porosity, pore size, and permeability, especially with respect to the interconnectivity of pores; resulting in a better understanding of drug release from pore-forming systems such as controlled release coatings. Additionally, quantification of film thickness may also be performed at the nanoscale, even with nanosized particles, as seen with lecithin coated silica particles in another study [120] This example demonstrates the possibility to even investigate nanometer sized coatings on nanoparticles. Colored coatings often contain inorganic pigments that are easily detected with back scattered electrons due to their higher atomic number. Such pigments should be evenly distributed in a coating for pharmaceutical elegance, or even from a functional perspective to allow sufficient protection from light for stability purposes [121]. FIB-SEM enables the imaging of even

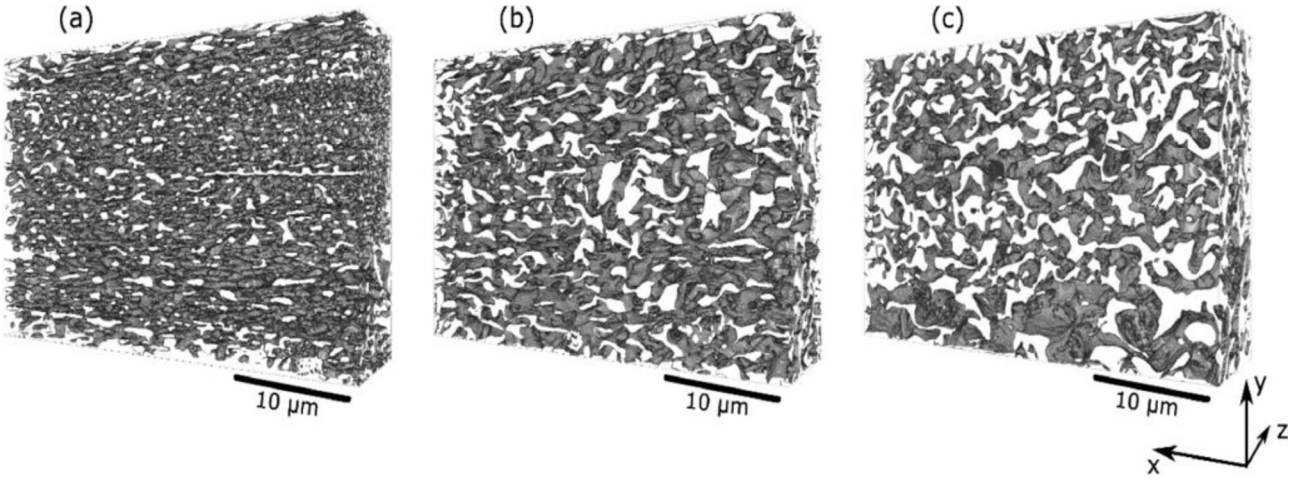

Fig. 7. 3D Reconstructed models of the porous controlled release coatings. Pores are displayed in white and pore walls in grey. Scaling with increased leached pore former from (a) to (c). Reprinted from [116] under the terms of the Creative Commons CC-BY license. Copyright 2021 Journal of Pharmaceutical Sciences.

nanosized pigments within the coating directly on DDS, without the risk of generating cutting artifacts that may be a result of rigid pigment particles within film, whilst avoiding complex sample preparation methods [122–124].

3.4. Particulates

3.4.1. Porous carriers for drug delivery

Porous structures are not only suitable as coatings for the controlled release of drugs, but are also found in excipients and carrier materials for the delivery of active ingredients, nutraceutical oils, or liquid formulations such as self-emulsifying drug delivery systems [125–128]. These carriers can consist of for example, mesoporous silica [28], functionalized calcium carbonate [129–131], or mesoporous magnesium carbonate [132,133]. Characterization of porous systems can be achieved using standard methods such as gas sorption analysis to obtain a quantitative description of surface area, or mercury intrusion porosimetry (MIP) to assess the radius of inlet pores in a sample. Although, MIP is a standard technique for determining the porosity of a sample, it is limited by the fact that only the size of the inlet pore can be determined and the pore shape is assumed to be cylindrical [134]. Furthermore, closed off or blocked pores can't be reached by MIP and therefore not detected. In addition, porous samples can be compressed by high pressures, which is especially true for soft materials [135]. Electron microscopy techniques, can help to substantiate the findings obtained by MIP, as EM allows the study of pore shape and size. As previously discussed, to gain access to the internal pores with SEM or TEM the samples must be broken or cut, since SEM analyzes only surfaces and TEM requires ultrathin samples. Mechanical breaking or cutting might be possible, especially for pure (drug free) excipient particles [136], but is often accompanied by the preparation problems described earlier. With FIB-SEM, even fine porous particles can be imaged without distorting the pore structure to reveal internal morphology and composition localization. Some fundamental studies have been carried out to investigate the relationship between MIP and FIB-SEM 2D image pore analysis with drug loaded functionalized calcium carbonate (FCC) carriers [129]. A further investigation has been conducted on proliposomal FCC carriers with the ability to form liposomes in situ [131]. The findings describe a data discrepancy between MIP and FIB-SEM with respect to pore size determination. This discrepancy was most likely due to the small sample size of the FIB-SEM data and the fact that the image processing was performed on 2D image data, as well as the complications regarding MIP use described above. However, it is possible to evaluate the inner particle structure as well as to distinguish between empty and filled pores. Following the investigations, the authors concluded that both methods should ideally be combined to adequality interpret the complex porous structures of the sample.

3.4.2. Spray dried particles

Another application for FIB includes the analysis of spray-dried particles. Depending on the spray drying conditions and the composition of the material, particles can have a variety of structural features. These features include among others spherical particles with solid, hollow or porous interiors [137]. The size ranges of many spray-dried particles are well suited for FIB-SEM studies. Early FIB-SEM studies have been performed on particles for inhalation; demonstrating the general suitability of the technique in this field. In these early studies, the authors particularly highlight the ability to visualize internal pores, since these are important for aerodynamic behavior [138]. FIB-SEM combined with micro-CT was applied to investigate spray dried hydroxypropylmethylcellulose-acetat-succinate (HPMC-AS) amorphous solid dispersions (ASD). The investigators correlated structural peculiarities, such as the size of the internal voids and particle wall thickness to the exhaust temperature of the spray-dried product. And, while micro-CT data was found to be more suitable for obtaining data sets that allow statistical evaluation of quantitative differences, FIB-SEM was found to provide more valuable information on the inner morphology well below the resolution of micro-CT [139]. An earlier study investigated the morphological properties of felodipine-polyvinylpyrrolidone ASD prepared by spray drying. They found intra batch morphological differences of the particles dependent on their particle size. The morphology shifted from a solid particle for the smallest particle size fraction, to increasingly nanoporous structures with larger particle size fractions. Additionally, it was found that large particles had felodipine enriched areas within particles which were confirmed by energy-dispersive spectroscopy (EDS), which allows the analyses of elemental composition using secondary X-rays generated from the sample after electron beam excitation. In this case, characteristic X-rays of chlorine were used to analyze felodipine distribution given that it was the only chlorine-containing substance in the particle [140]. Another recent study used the FIB-SEM technique to assess the internal structure of spray dried powdered vaccines. In this study the investigators were able to link the interparticle surface to viral activity loss. The larger the surface area of the particle, especially the interparticle voids, the lower the viral activity. [59].

4. Applications of broad ion beam preparations in drug delivery

Limitations described above regarding cross-section size are not as applicable for BIB milling, and as a result larger samples may be prepared with an increased cross section size; as compared to FIB-SEM. Nevertheless, the technique has not been regularly applied in pharmaceutical science, but early investigations provide interesting results and insights. Previously, the FDA assessed the BIB technique under cryogenic conditions, as a tool for PLGA microsphere investigation of ARESTIN® (minocycline hydrochloride microspheres) [37]. They concluded that the method could indeed be used to determine microstructural equivalence between the reference listed drug and a generic equivalent product, and that it was especially useful in regard to complex DDS such as PLGA microspheres. Another investigation using BIB milling, investigated polymer nanoparticles prepared using a double-emulsion technique loaded with gold labeled bovine serum albumin (BSA). The study revealed that the postulated internal structure was only detectable above a certain nanoparticle diameter [33] (Fig. 8). As shown in the overview image of the cross-section (Fig. 8a), a BIB instrument was used to mill a wafer (bright area) with dispersed nanoparticles on its surface (grayish spheres). Looking at the higher magnification image (Fig. 8B), bright spots of gold labeled BSA are visible only on the surfaces, but not within the particles.

5. Drug delivery systems in biological environments

FIB-SEM studies can be used to analyze various biopharmaceutical processes, such as the uptake of colloidal carriers, or the interaction of tissues and cells with the substrates on which they grow. Imaging drug delivery phenomena at relevant biological barriers or targets will ultimately deepen our understanding of the underlaying mechanisms of drug transport and beyond.

5.1. High resolution investigations of biological barriers

In addition to the application of FIB-SEM tomography in the direct context of drug delivery, the technique can provide valuable insights into structural biology that can benefit the understanding of biological drug barriers, and thus how to overcome them. The better the understanding of such barriers, either in healthy or diseased states, the better drug carriers and model systems can be developed to meet patient needs [141,142]. Tissues, cells, or ex vivo models being investigated include for example, alveolar epithelia cells [143], glomerular epithelia cells [144], skin [145,146], neuronal tissue [147,148], cornea [149,150] and bovine hoof sheets as an ex vivo model for permeation studies [151].

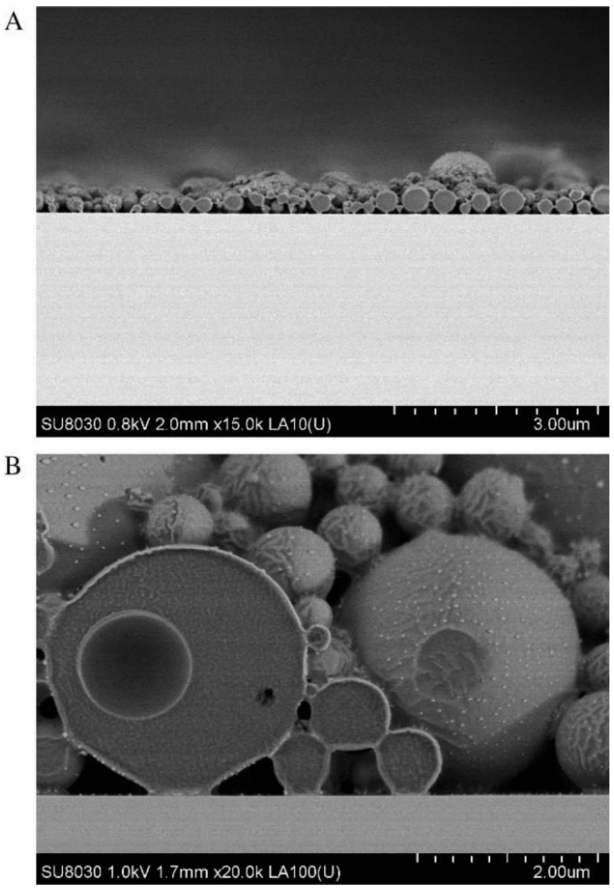

Fig. 8. Broad ion beam milled PLGA nanoparticles containing gold labeled BSA dispersed on a wafer (Fig. 8 A). The gold labeled BSA is seen as bright dots on the surface (Fig. 8B). Reprinted from [33] with permission from Elsevier. Copyright (2015) European Journal of Pharmaceutics and Biopharmaceutics.

5.2. Colloidal carrier interaction with cells and tissues

Another interesting research field is the study of the interaction of drug delivery systems with biological systems, particularly using FIB-SEM tomography. Most studies in this area have been conducted using inorganic materials because standard lipid- or polymer-based materials are either soluble in the solvents used for standard EM sample preparation procedures, or are difficult to observe due to their composition of low atomic weight elements; providing little contrast for distinguishing them from the surrounding sample material. FIB-SEM allows high-resolution imaging of particle uptake into cells, analysis of their intracellular fate, and localization using tomography. The interaction of drug-loaded PLGA-based multi-metallic polymeric microparticles with *mycobacterium tuberculosis* in THP1-macrophages has been investigated using FIB-SEM and other electron microscopy based techniques [152]. The investigators described various interesting aspects about sample preparation and particle uptake. In these studies, a Quetol-based EM embedding resin was used which dissolved the PLGA from the microparticles during the embedding process, whereas a hydrophilic Unicryl resin allowed the identification of the PLGA (as it did not dissolve the PLGA microparticles within the cells), but the PLGA still had low contrast. These methods made it possible to image multi metallic polymer particle influence on intracellular located *Mycobacterium tuberculosis* cells, resulting in increased rifampicin potency due to a decrease in bacterium cellular membrane integrity. Another study, employed FIB-SEM tomography as a technique to image nanoparticle uptake using non-functionalized gold nanoparticles on primary human umbilical vein endothelial cells. The data from this study indicated that the particles were most likely located in *endo-* or lysosomes within the cells, with a tendency to aggregate within these organelles. These organelles we shown to be clearly visible and distributed over the cellular volume as nearly all contained some amount of gold [153]. Most FIB-SEM studies have only performed cross-sections with 2D imaging, and have not investigated the uptake of the particles using 3D models. In general, particles used in localization studies have consisted of for example, silver [152,154], gold [153,155,156], or iron oxides [157,158]. It should be noted that most of the data related to the fate of intracellular particle uptake has been performed using TEM studies with such 2D images.

5.3. Interaction between surfaces with cells and tissues

In addition to the importance of interactions between nanoscale particles and biological systems, it is also important to consider interactions of biological systems (e.g. with regard to biocompatibility) with larger particles or materials such as implants, stents, microneedles, or scaffolds used in tissue engineering. FIB-SEM can allow direct cross-sectional imaging of cells and tissues interacting with such substrates. Many of the aforementioned samples have properties that can make it difficult to obtain high-resolution cross-sections or 3D structures, as embedding processes could alter a given structure, potentially due to its physical instability [159]. On the other hand, some cell penetrating needles are composed of material which is challenging to cut by means of ultramicrotomy due to their hardness. Using FIB-SEM, it is possible to reconstruct osteoblasts grown on electro spun PLGA fibers at high resolution in 3D [160], which would have been difficult to prepare using a different method due to its complex composition and softness. Another application demonstrating the capability of the FIB-SEM technique, is the fabrication of clean cross sections of nano and microneedles and their penetration of cells, e.g. for ex vivo gene manipulation [161,162]. In this example, the needles (comprising silicon dioxide a hard material) are difficult to cut, as a composite using ultramicrotomy, since there is risk of sample delamination or damage to the microtomy knives themselves [163].

6. What are the challenges of FIB-SEM in drug delivery?

Even though the use of FIB-SEM has long been established in semiconductor science, and its outstanding imaging capabilities are proven in structural biology, its application in pharmaceutics is still sparse. The implementation of FIB-SEM within structural biology was achieved quickly because sample preparation protocols, especially for TEM investigations, had already been established long ago. FIB-SEM or other advanced EM techniques used in pharmaceutics still need to be adapted to existing techniques from materials science and biology to adequately address issues such as localization of DDS in cells/tissues. This is especially true in areas such as contrast generation and fixation, as most excipients/API do not have large differences in terms of average atomic number.

6.1. Challenges in drug delivery

With little exploration to-date, another highly relevant field of application is that of intracellular localization of lipoid or polymeric pharmaceutical excipients by means of EM, since light microscopy methods are more commonly used for imaging intracellular trafficking [164,165]. This is particularly relevant for intracellular delivery of sensitive APIs such as RNA, DNA [166–168], or proteins [169,170] that need access to the intracellular space for successful administration. However, most EM based cellular uptake studies have been performed with inorganic nanoparticles, since these already have highly electron dense properties and are not affected by most of the chemicals used in the fixation and staining of cells or are rapidly digested. Thus, a major challenge when investigating polymeric or lipid-based DDS is the lack of sample preparation protocols suitable in preserving both cellular

ultrastructure and particle morphology, while enabling the visualization of uptake and trafficking of the drug delivery vehicle with the electron microscope. Before issues of nanoparticle uptake and localization in cells and tissues can be comprehensively addressed, appropriate protocols must be developed to ensure that the DDS and the respective biological materials retain their ultrastructural properties, whilst exhibiting sufficient contrast. There will most likely be cases where it won't t be possible to retain both cellular ultrastructure and particle morphology. A promising approach to truly elucidate the localization of DDS within cells may be new techniques such as correlative light and electron microscopy (CLEM). [171–174]

6.1.1. Correlative light and electron microscopy (CLEM) as possible solution

CLEM is an approach in which the same cellular ROI can be visualized using light microscopy (often using some form of super resolution microscopy), before being subsequently imaged using electron microscopy [175]. This approach allows rapid screening of a sample initially using light microscopy to enable the tracking of, for example, a fluorescent-labeled component. A technique such as FIB-SEM or EM in general can then be used to image the same location. This correlative approach makes it possible to overlay both images. Here, it would still be possible to obtain the localization of the drug delivery system by its fluorescent label and to put this signal into an ultrastructural context after EM imaging. Suitable EM techniques could be TEM or FIB-SEM. FIB-SEM would allow correlation of fluorescence and EM ultrastructure in a combined 3D model. Such an approach could also provide information on whether the fluorescent tracer is still present in the DDS of interest or has been removed from the DDS, e.g., by digestion.

7. Potential of FIB-SEM in drug delivery

The use of FIB-SEM as a tool for characterizing long-acting PLGA-based injectable drugs and implants was recently evaluated by the FDA Center for Drug Evaluation and Research [37,176]. It was concluded that an ion beam prepared cross-section may be used to determine microstructural equivalency of PLGA-based microspheres, when comparing a generic drug product against a reference listed drug. This conclusion could be extended to a wider range of drug delivery systems whose microstructural characteristics are also critical to their performance. Many advanced drug delivery systems are complex in design, and may be sensitive to variation in manufacturing, for example for the various types of micro- or nano-capsules that have been used or investigated. It is therefore important to verify the presumed structure of such drug delivery systems following their manufacture. It follows that If the actual structure does not match the anticipated one, then the assumed mode of action of the delivery system could be incorrect. Indeed, FIB-SEM has the potential to analyze these types of microstructural features with unprecedented precision, challenging the *status quo* in many aspects of drug delivery, because many hitherto unobtainable critical properties could be assessed in the final manufactured drug product. These properties, especially when nanosized, are often difficult to observe by other means and, are thus regularly neglected or ignored. In general, FIB-SEM may also be the most versatile and suitable electron microscopy-based volume imaging method for pharmaceutical samples, due to the largely material-independent milling process, as most other preparation techniques require an ultramicrotomy approach [177,178].

The potential of FIB-SEM is not limited to the analysis of drug delivery. As described above, the ability to analyze biological materials in 3D will improve understanding of nanoparticle uptake, particularly by combining light and electron microscopy techniques in a CLEM approach. FIB-SEM tomography can be used to describe the relationship between nanoparticles and cell organelles, especially for single cells or small cell clusters [179]. In general, electron microscopy techniques are better suited for imaging nanoparticles in a cellular context than standard light microscopy techniques, as EM can be used to image a single cell down to their ultrastructural details [180]. This becomes apparent, as organelles can stretch over vast distances (in a cellular context), and possess dynamic morphological features. Imaging becomes even more complex when one considers aspects such as, cellular uptake and cellular degradation pathways like endocytosis and autophagy. Many of these organelles can only be characterized by their membrane organization using electron microscopy [165,181]. When nanoparticles are taken up by the cell by endocytosis, they may also trigger autophagy [182–185]. However, both processes can be consolidated when an autophagosome fuses with a late endosome leading to the formation of an amphisome [181,186] (containing both organelles and nanoparticles [187]) which is destined for degradation. Various studies have aimed to determine the co-localization of stained nanoparticles with intracellular organelles using light microscopy techniques. However, such stained structures may have already encountered one another within an amphisome, giving a false impression of successful drug delivery. It is therefore important to visualize the cellular structures in detail to ensure that the particles are co-localized at the correct target; a possibility using electron microscopy [173,174]. In this context, only EM can distinguish organelles by their morphology or membrane organization, as well as the particles themselves and their interactions [188]. In general, great caution should be taken when interpreting such images, as cells are capable of digesting pharmaceutical excipients and thus altering the expected DDS structure or forming vesicular structures such as lipid droplets or exosomes. Especially exosomes can easily be mistaken for liposomes or nanoemulsion droplets (Fig. 9B).

FIB-SEM enables nanoparticle distribution studies over a whole cell or a larger cellular volume, highlighting specific locations across various organelles as well as their physical state for an accurate assessment of the functional principles. Depending on the proposed mode of delivery, only EM-based techniques have the necessary resolution to demonstrate that the drug delivery system reaches the target structure intact. EM examinations cannot prove the successful delivery of the API, nor can it negate previous results with positive treatment outcomes, as these results are obtained with quantitative techniques that analyze the effect of an API. However, microscopy could allow the effect of the drug delivery system to be linked to its cellular localization. And, it may be possible to achieve the proposed effect without the suggested delivery mechanism. Nuclear delivery is such an example, where intranuclear presence or just being in outside vicinity of the nuclear membrane can lead to ambiguous interpretations. A light microscopy technique, especially a non-super resolution based technique, could be used to suggest particle localization in a cell nucleus, although the particle might actually just be in a nuclear envelope invagination [189–192] (Fig. 9A).

Recently, several approaches have been tested for different DDSs such as liposomes, chitosan nanoparticles, or ethosomes [180,193–197] that take advantage of the affinity of EM contrast agents towards excipients in these DDS. An optimal method would contrast the drug delivery system material itself without affecting cellular ultrastructure, or better yet, contrast the biological material during the same process.

8. Conclusions

FIB-SEM has proven its value in pharmaceutical research, especially in recent years with a focus on the characterization of DDS. Nanoscale characterization of advanced DDS is of immense importance to draw conclusions about the mechanism of action. FIB-SEM is the most suitable volume electron microscopy technique for pharmaceutics, because it is capable of being used to analyze both DDS and biological samples due to its capacity for material-independent ion beam milling. Other volume electron microscopy techniques, while beneficial for biological sample analysis, are less suitable for analysis of DDS due to their dependance on ultramicrotomy. The study of nanoparticle uptake in cells and their respective localization in a cellular environment is of high interest, however, these studies usually rely on light microscopy techniques or inorganic electron dense particles for EM studies. Therefore, FIB-SEM

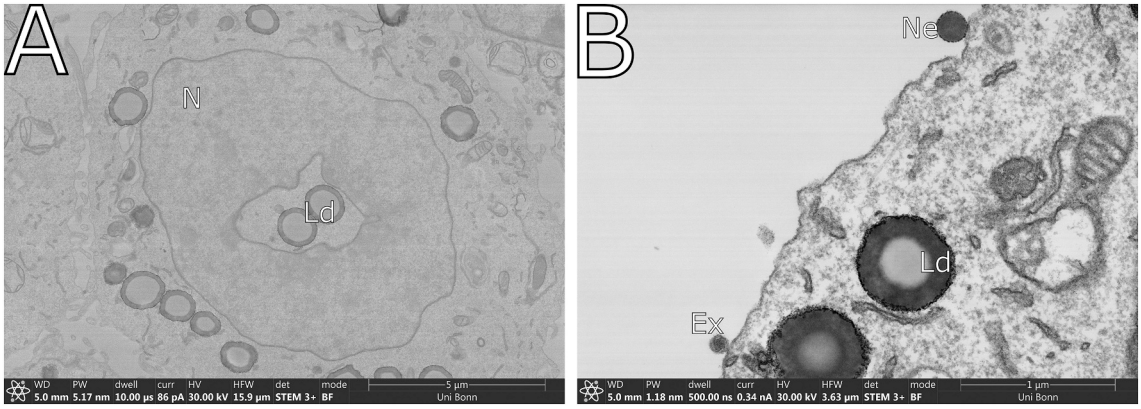

Fig. 9. Bright field scanning transmission electron micrographs of macrophages after treatment with nanoemulsions. Image section A shows a nuclear invagination with cytosol and lipid droplets (Ld) surrounded by the nucleus (N). These lipid droplets are formed by the cell itself after complete digestion of the nanoemulsion. Consequently, the lipid droplets are serving as cellular lipid storage organelles. In comparison to the lipid droplets, the primary delivery system is visible in section B as undigested nanoemulsion droplet (Ne) attached to the cell surface. Also visible in section B is the morphological difference between undigested nanoemulsion droplets (Ne) and the exosome (Ex), which also contains electron-dense material but is surrounded by a brighter lipid bilayer and is formed by the cell itself. (unpublished data).

has the potential to play an extraordinary role in the future in studying the interaction of DDS with their respective targets, as well as uncovering structural features within advanced DDS.

CRediT authorship contribution statement

Thilo Faber: Writing – original draft, Conceptualization. **Jason T. McConville:** Writing – review & editing. **Alf Lamprecht:** Writing – review & editing, Resources, Conceptualization.

Data availability

Data will be made available on request.

References

[1] E. Betzig, S.W. Hell, W.E. Moerner, The Nobel Prize in Chemistry 2014, (n.d.) 1.
[2] J. Dubochet, J. Frank, R. Henderson, The Nobel Prize in Chemistry 2017, (n.d.) 1.
[3] N. Fleming, The microscopic advances that are opening big opportunities in cell biology, Nature. 575 (2019) S91–S94, https://doi.org/10.1038/d41586-019-03650-w.
[4] W. Kühlbrandt, The resolution revolution, Science. 343 (2014) 1443–1444, https://doi.org/10.1126/science.1251652.
[5] R.A. Carlton, Pharmaceutical Microscopy, Springer New York, New York, NY, 2011, https://doi.org/10.1007/978-1-4419-8831-7.
[6] D. Pinotsi, S. Rodighiero, S. Campioni, G. Csucs, An easy path for correlative Electron and super-resolution light microscopy, Sci. Rep. 9 (2019) 15526, https://doi.org/10.1038/s41598-019-52047-2.
[7] A. Ostrowski, D. Nordmeyer, A. Boreham, C. Holzhausen, L. Mundhenk, C. Graf, M.C. Meinke, A. Vogt, S. Hadam, J. Lademann, E. Rühl, U. Alexiev, A.D. Gruber, Overview about the localization of nanoparticles in tissue and cellular context by different imaging techniques, Beilstein J. Nanotechnol. 6 (2015) 263–280, https://doi.org/10.3762/bjnano.6.25.
[8] T. Ando, S.P. Bhamidimarri, N. Brending, H. Colin-York, L. Collinson, N.D. Jonge, P.J. de Pablo, E. Debroye, C. Eggeling, C. Franck, M. Fritzsche, H. Gerritsen, B.N. G. Giepmans, K. Grunewald, J. Hofkens, J.P. Hoogenboom, K.P.F. Janssen, R. Kaufmann, J. Klumperman, N. Kurniawan, J. Kusch, N. Liv, V. Parekh, D. B. Peckys, F. Rehfeldt, D.C. Reutens, M.B.J. Roeffaers, T. Salditt, I.A.T. Schaap, U. S. Schwarz, P. Verkade, M.W. Vogel, R. Wagner, M. Winterhalter, H. Yuan, G. Zifarelli, The 2018 correlative microscopy techniques roadmap, J. Phys. D. Appl. Phys. 51 (2018) 443001, https://doi.org/10.1088/1361-6463/aad055.
[9] J.D. Clogston, V.A. Hackley, A. Prina-Mello, S. Puri, S. Sonzini, P.L. Soo, Sizing up the next generation of nanomedicines, Pharm. Res. 37 (2019) 6, https://doi.org/10.1007/s11095-019-2736-y.
[10] E.J. Guggenheim, A. Khan, J. Pike, L. Chang, I. Lynch, J.Z. Rappoport, Comparison of confocal and super-resolution reflectance imaging of metal oxide nanoparticles, PLoS One 11 (2016) e0159980, https://doi.org/10.1371/journal.pone.0159980.
[11] M.W. Tuijtel, A.J. Koster, S. Jakobs, F.G.A. Faas, T.H. Sharp, Correlative cryo super-resolution light and electron microscopy on mammalian cells using fluorescent proteins, Sci. Rep. 9 (2019) 1369, https://doi.org/10.1038/s41598-018-37728-8.
[12] A. Reisch, A.S. Klymchenko, Fluorescent polymer nanoparticles based on dyes: seeking brighter tools for bioimaging, Small. 12 (2016) 1968–1992, https://doi.org/10.1002/smll.201503396.
[13] K. Trofymchuk, J. Valanciunaite, B. Andreiuk, A. Reisch, M. Collot, A. S. Klymchenko, BODIPY-loaded polymer nanoparticles: chemical structure of cargo defines leakage from nanocarrier in living cells, J. Mater. Chem. B 7 (2019) 5199–5210, https://doi.org/10.1039/C8TB02781A.
[14] A.S. Klymchenko, F. Liu, M. Collot, N. Anton, Dye-loaded Nanoemulsions: biomimetic fluorescent Nanocarriers for bioimaging and nanomedicine, Adv. Healthc. Mater. 10 (2021) 2001289, https://doi.org/10.1002/adhm.202001289.
[15] S. Snipstad, S. Hak, H. Baghirov, E. Sulheim, Ý. Mørch, S. Lélu, E. von Haartman, M. Bäck, K.P.R. Nilsson, A.S. Klymchenko, C. de Lange Davies, A.K.O. Åslund, Labeling nanoparticles: dye leakage and altered cellular uptake, Cytometry A 91 (2017) 760–766, https://doi.org/10.1002/cyto.a.22853.
[16] Y.V. Pathak, V.D. Labhashetwar, Evaluation of Drug Delivery Systems by Electron Microscopy Techniques, (n.d.) 17.
[17] S. Sadamatsu, M. Tanaka, K. Higashida, S. Matsumura, Transmission electron microscopy of bulk specimens over 10μm in thickness, Ultramicroscopy. 162 (2016) 10–16, https://doi.org/10.1016/j.ultramic.2015.09.001.
[18] M.D. Eddleston, E.G. Bithell, W. Jones, Transmission Electron microscopy of pharmaceutical materials, J. Pharm. Sci. 99 (2010) 4072–4083, https://doi.org/10.1002/jps.22220.
[19] R.G. Ricarte, T.P. Lodge, M.A. Hillmyer, Detection of pharmaceutical drug crystallites in solid dispersions by transmission Electron microscopy, Mol. Pharm. 12 (2015) 983–990, https://doi.org/10.1021/mp500682x.
[20] J. Vastenhout, H. Gnaegi, Ultramicrotomy of polymers using an oscillating diamond knife, Improv. Poly. Morphol. Microsc. Microanal. 8 (2002) 324–325, https://doi.org/10.1017/S1431927602100560.
[21] J. Stoiber, W.H. Muss, G. Pohla-Gubo, J. Ruckhofer, G. Grabner, Histopathology of human corneas after amniotic membrane and Limbal stem cell transplantation for severe chemical burn, Cornea. 21 (2002) 482.
[22] S. Velamoor, A. Mitchell, M. Bostina, D. Harland, Processing hair follicles for transmission electron microscopy, Exp. Dermatol. 31 (2022) 110–121, https://doi.org/10.1111/exd.14439.
[23] V. Klang, C. Valenta, N.B. Matsko, Electron microscopy of pharmaceutical systems, Micron. 44 (2013) 45–74, https://doi.org/10.1016/j.micron.2012.07.008.
[24] R. Nordström, L. Zhu, J. Härmark, Y. Levi-Kalisman, E. Koren, Y. Barenholz, G. Levinton, D. Shamrakov, Quantitative Cryo-TEM reveals new structural details of Doxil-like PEGylated liposomal doxorubicin formulation, Pharmaceutics. 13 (2021) 123, https://doi.org/10.3390/pharmaceutics13010123.
[25] V. Klang, N.B. Matsko, C. Valenta, F. Hofer, Electron microscopy of nanoemulsions: an essential tool for characterisation and stability assessment, Micron. 43 (2012) 85–103, https://doi.org/10.1016/j.micron.2011.07.014.
[26] M. Colomb-Delsuc, R. Raim, C. Fiedler, S. Reuberger, J. Lengler, R. Nordström, M. Ryner, I.M. Folea, B. Kraus, J.A. Hernandez Bort, I.-M. Sintorn, Assessment of the percentage of full recombinant adeno-associated virus particles in a gene therapy drug using CryoTEM, PLoS One 17 (2022) e0269139, https://doi.org/10.1371/journal.pone.0269139.
[27] T. Ehtezazi, C. Washington, C.D. Melia, Determination of the internal morphology of poly (D,L-lactide) microspheres using stereological methods, J. Control. Release 57 (1999) 301–314, https://doi.org/10.1016/S0168-3659(98)00118-7.
[28] A. Baumgartner, O. Planinšek, Application of commercially available mesoporous silica for drug dissolution enhancement in oral drug delivery, Eur. J. Pharm. Sci. 167 (2021) 106015, https://doi.org/10.1016/j.ejps.2021.106015.

[29] S. Zhang, D. Wu, L. Zhou, Characterization of controlled release microspheres using FIB-SEM and image-based release prediction, AAPS PharmSciTech 21 (2020) 194, https://doi.org/10.1208/s12249-020-01741-w.
[30] S. Zhang, K. Nagapudi, M. Shen, J. Lomeo, Y. Qin, A. Zhu, P. Nayak, D. Chang, R. N. Hannoush, Release mechanisms and practical percolation threshold for long-acting biodegradable implants: an image to simulation study, J. Pharm. Sci. (2021), https://doi.org/10.1016/j.xphs.2021.12.009. S0022354921006821.
[31] Z. Liu, L. Li, S. Zhang, J. Lomeo, A. Zhu, J. Chen, S. Barrett, A. Koynov, S. Forster, P. Wuelfing, W. Xu, Correlative image-based release prediction and 3D microstructure characterization for a long acting parenteral implant, Pharm. Res. (2021), https://doi.org/10.1007/s11095-021-03145-2.
[32] A.G. Clark, R. Wang, Y. Qin, Y. Wang, A. Zhu, J. Lomeo, Q. Bao, D.J. Burgess, J. Chen, B. Qin, Y. Zou, S. Zhang, Assessing microstructural critical quality attributes in PLGA microspheres by FIB-SEM analytics, J. Control. Release 349 (2022) 580–591, https://doi.org/10.1016/j.jconrel.2022.06.066.
[33] D. Francis, S. Mouftah, R. Steffen, A. Beduneau, Y. Pellequer, A. Lamprecht, Ion milling coupled field emission scanning electron microscopy reveals current misunderstanding of morphology of polymeric nanoparticles, Eur. J. Pharm. Biopharm. 89 (2015) 56–61, https://doi.org/10.1016/j.ejpb.2014.11.008.
[34] A. Rübe, G. Hause, K. Mäder, J. Kohlbrecher, Core-shell structure of Miglyol/poly (d,l-lactide)/Poloxamer nanocapsules studied by small-angle neutron scattering, J. Control. Release 107 (2005) 244–252, https://doi.org/10.1016/j.jconrel.2005.06.005.
[35] T. Nassar, A. Rom, A. Nyska, S. Benita, Novel double coated nanocapsules for intestinal delivery and enhanced oral bioavailability of tacrolimus, a P-gp substrate drug, J. Control. Release 133 (2009) 77–84, https://doi.org/10.1016/j.jconrel.2008.08.021.
[36] Y.K. Tak, S. Pal, P.K. Naoghare, S. Rangasamy, J.M. Song, Shape-dependent skin penetration of silver nanoparticles: does it really matter? Sci. Rep. 5 (2015) 16908, https://doi.org/10.1038/srep16908.
[37] Y. Ma, J. Liang, J. Zheng, Y. Wang, M. Ashraf, C. Srinivasan, Significance of cryogenic broad ion beam milling in evaluating microstructures of PLGA-based drug products, Microsc. Microanal. 27 (2021) 90–91, https://doi.org/10.1017/S1431927621000945.
[38] O. Lambert, O. Nagele, V. Loux, J.-D. Bonny, L. Marchal-Heussler, Poly(ethylene carbonate) microspheres: manufacturing process and internal structure characterization, J. Control. Release 67 (2000) 89–99, https://doi.org/10.1016/S0168-3659(00)00198-X.
[39] G. Ruan, S.-S. Feng, Q.-T. Li, Effects of material hydrophobicity on physical properties of polymeric microspheres formed by double emulsion process, J. Control. Release 84 (2002) 151–160, https://doi.org/10.1016/S0168-3659(02)00292-4.
[40] J. Wang, B.M. Wang, S.P. Schwendeman, Characterization of the initial burst release of a model peptide from poly(d,l-lactide-co-glycolide) microspheres, J. Control. Release 82 (2002) 289–307, https://doi.org/10.1016/S0168-3659(02)00137-2.
[41] T. Hatano, S. Nakaba, Y. Horikawa, R. Funada, A combination of scanning electron microscopy and broad argon ion beam milling provides intact structure of secondary tissues in woody plants, Sci. Rep. 12 (2022) 9152, https://doi.org/10.1038/s41598-022-13122-3.
[42] G.H. Michler, Preparation of Thin Sections: (Cryo)ultramicrotomy and (Cryo) microtomy, in: Electron Microscopy of Polymers, Springer, Berlin, Heidelberg, 2008, pp. 199–217, https://doi.org/10.1007/978-3-540-36352-1_11.
[43] P. Blasi, Poly(lactic acid)/poly(lactic-co-glycolic acid)-based microparticles: an overview, J. Pharm. Investig. 49 (2019) 337–346, https://doi.org/10.1007/s40005-019-00453-z.
[44] F. Siepmann, V. Le Brun, J. Siepmann, Drugs acting as plasticizers in polymeric systems: a quantitative treatment, J. Control. Release 115 (2006) 298–306, https://doi.org/10.1016/j.jconrel.2006.08.016.
[45] M. Mamusa, R. Mastrangelo, T. Glen, S. Murgia, G. Palazzo, J. Smets, P. Baglioni, Rational Design of Sustainable Liquid Microcapsules for spontaneous fragrance encapsulation, Angew. Chem. Int. Ed. 60 (2021) 23849–23857, https://doi.org/10.1002/anie.202110446.
[46] N. Koifman, Y. Talmon, Cryogenic Electron microscopy methodologies as analytical tools for the study of self-assembled pharmaceutics, Pharmaceutics. 13 (2021) 1015, https://doi.org/10.3390/pharmaceutics13071015.
[47] V. Tournier-Lasserve, A. Boudet, P. Sopéna, Artefacts and their healing in ultramicrotomy of side-chain liquid-crystal polymers, Ultramicroscopy. 58 (1995) 123–130, https://doi.org/10.1016/0304-3991(94)00203-Y.
[48] J. Orloff, M. Utlaut, L. Swanson, High Resolution Focused Ion Beams: FIB and its Applications, Springer US, Boston, MA, 2003, https://doi.org/10.1007/978-1-4615-0765-9.
[49] H.M. Urbassek, Chapter 17 sputtering and laser ablation, in: E. Hasselbrink, B. I. Lundqvist (Eds.), Handbook of Surface Science, North-Holland, 2008, pp. 871–913, https://doi.org/10.1016/S1573-4331(08)00017-6.
[50] B.V. King, J.F. Moore, Y. Cui, I.V. Veryovkin, C.E. Tripa, Comparison of laser ablation and sputter desorption of clusters from Au7Cu5Al4, Nucl. Instrum. Methods Phys. Res., Sect. B 340 (2014) 72–75, https://doi.org/10.1016/j.nimb.2014.07.039.
[51] M.P. Echlin, A. Mottura, C.J. Torbet, T.M. Pollock, A new TriBeam system for three-dimensional multimodal materials analysis, Rev. Sci. Instrum. 83 (2012) 023701, https://doi.org/10.1063/1.3680111.
[52] W.L. Rice, A.N.V. Hoek, T.G. Păunescu, C. Huynh, B. Goetze, B. Singh, L. Scipioni, L.A. Stern, D. Brown, High resolution helium ion scanning microscopy of the rat kidney, PLoS One 8 (2013) e57051, https://doi.org/10.1371/journal.pone.0057051.
[53] M.S. Joens, C. Huynh, J.M. Kasuboski, D. Ferranti, Y.J. Sigal, F. Zeitvogel, M. Obst, C.J. Burkhardt, K.P. Curran, S.H. Chalasani, L.A. Stern, B. Goetze, J.A. J. Fitzpatrick, Helium ion microscopy (HIM) for the imaging of biological samples at sub-nanometer resolution, Sci. Rep. 3 (2013) 3514, https://doi.org/10.1038/srep03514.
[54] N. Klingner, G. Hlawacek, P. Mazarov, W. Pilz, F. Meyer, L. Bischoff, Imaging and milling resolution of light ion beams from helium ion microscopy and FIBs driven by liquid metal alloy ion sources, Beilstein J. Nanotechnol. 11 (2020) 1742–1749, https://doi.org/10.3762/bjnano.11.156.
[55] L.A. Giannuzzi, F.A. Stevie (Eds.), Introduction to Focused Ion Beams: Instrumentation, Theory, Techniques, and Practice, Springer, New York, 2005.
[56] N.D. Bassim, B.T. De Gregorio, A.L.D. Kilcoyne, K. Scott, T. Chou, S. Wirick, G. Cody, R.M. Stroud, Minimizing damage during FIB sample preparation of soft materials, J. Microsc. 245 (2012) 288–301, https://doi.org/10.1111/j.1365-2818.2011.03570.x.
[57] S.H. Moghadam, R. Dinarvand, L.H. Cartilier, The focused ion beam technique: a useful tool for pharmaceutical characterization, Int. J. Pharm. 321 (2006) 50–55, https://doi.org/10.1016/j.ijpharm.2006.05.006.
[58] C. Janich, A. Friedmann, J. Martins de Souza e Silva, C. Santos De Oliveira, L. E. de Souza, D. Rujescu, C. Hildebrandt, M. Beck-Broichsitter, C.E.H. Schmelzer, K. Mäder, Risperidone-loaded PLGA–lipid particles with improved release kinetics: manufacturing and detailed characterization by Electron microscopy and Nano-CT, Pharmaceutics. 11 (2019) 665, https://doi.org/10.3390/pharmaceutics11120665.
[59] V. Singh, B.A. Morgan, A. Schertel, M. Dolovich, Z. Xing, M.R. Thompson, E. D. Cranston, Internal microstructure of spray dried particles affects viral vector activity in dry vaccines, Int. J. Pharm. 640 (2023) 122988, https://doi.org/10.1016/j.ijpharm.2023.122988.
[60] C. Kizilyaprak, J. Daraspe, B.M. Humbel, Focused ion beam scanning electron microscopy in biology: FOCUSED ION BEAM SCANNING ELECTRON MICROSCOPY, J. Microsc. 254 (2014) 109–114, https://doi.org/10.1111/jmi.12127.
[61] C. Kizilyaprak, Y.-D. Stierhof, B.M. Humbel, Volume microscopy in biology: FIB-SEM tomography, Tissue Cell 57 (2019) 123–128, https://doi.org/10.1016/j.tice.2018.09.006.
[62] J. Kuo (Ed.), Electron Microscopy: Methods and Protocols, Third edition, Humana Press, New York, 2014.
[63] A.M. Steyer, A. Schertel, C. Nardis, W. Möbius, FIB-SEM of mouse nervous tissue: Fast and slow sample preparation, in: Methods in Cell Biology, Elsevier, 2019, pp. 1–21, https://doi.org/10.1016/bs.mcb.2019.03.009.
[64] A.A. Polilov, A.A. Makarova, S. Pang, C. Shan Xu, H. Hess, Protocol for preparation of heterogeneous biological samples for 3D electron microscopy: a case study for insects, Sci. Rep. 11 (2021) 4717, https://doi.org/10.1038/s41598-021-83936-0.
[65] K.A. Telari, B.R. Rogers, H. Fang, L. Shen, R.A. Weller, D.N. Braski, Characterization of platinum films deposited by focused ion beam-assisted chemical vapor deposition, J. Vac. Sci. Technol. B 20 (2002) 590, https://doi.org/10.1116/1.1458958.
[66] N. Schieber, P. Machado, S. Markert, C. Stigloher, Y. Schwab, A. Steyer, Minimal resin embedding of multicellular specimens for targeted FIB-SEM imaging, Microsc. Microanal. 23 (2017) 1274–1275, https://doi.org/10.1017/S1431927617007036.
[67] A.M. Steyer, T. Ruhwedel, W. Möbius, Biological sample preparation by high-pressure freezing, microwave-assisted contrast enhancement, and minimal resin embedding for volume imaging, JoVE (J. Visual. Exper.). (2019) e59156, https://doi.org/10.3791/59156.
[68] T. Pingel, M. Skoglundh, H. Grönbeck, E. Olsson, Revealing local variations in nanoparticle size distributions in supported catalysts: a generic TEM specimen preparation method, J. Microsc. 260 (2015) 125–132, https://doi.org/10.1111/jmi.12274.
[69] C.D.J. Parmenter, M.W. Fay, C. Hartfield, H.M. Eltaher, Making the practically impossible “merely difficult”—cryogenic FIB lift-out for “damage free” soft matter imaging, Microsc. Res. Tech. 79 (2016) 298–303, https://doi.org/10.1002/jemt.22630.
[70] R.M. Langford, C. Clinton, In situ lift-out using a FIB-SEM system, Micron. 35 (2004) 607–611, https://doi.org/10.1016/j.micron.2004.03.002.
[71] J. Klaver, S. Hemes, M. Houben, G. Desbois, Z. Radi, J.L. Urai, The connectivity of pore space in mudstones: insights from high-pressure Wood’s metal injection, BIB-SEM imaging, and mercury intrusion porosimetry, Geofluids. 15 (2015) 577–591, https://doi.org/10.1111/gfl.12128.
[72] J. Klaver, G. Desbois, J.L. Urai, R. Littke, BIB-SEM study of the pore space morphology in early mature Posidonia shale from the Hils area, Germany, Int. J. Coal Geol. 103 (2012) 12–25, https://doi.org/10.1016/j.coal.2012.06.012.
[73] J. Klaver, G. Desbois, R. Littke, J.L. Urai, BIB-SEM pore characterization of mature and post mature Posidonia shale samples from the Hils area, Germany, Int. J. Coal Geol. 158 (2016) 78–89, https://doi.org/10.1016/j.coal.2016.03.003.
[74] M.E. Houben, G. Desbois, J.L. Urai, Pore morphology and distribution in the Shaly facies of Opalinus clay (Mont Terri, Switzerland): insights from representative 2D BIB–SEM investigations on mm to nm scale, Appl. Clay Sci. 71 (2013) 82–97, https://doi.org/10.1016/j.clay.2012.11.006.
[75] S. Giffin, R. Littke, J. Klaver, J.L. Urai, Application of BIB–SEM technology to characterize macropore morphology in coal, Int. J. Coal Geol. 114 (2013) 85–95, https://doi.org/10.1016/j.coal.2013.02.009.
[76] T. Takamizawa, A. Imai, E. Hirokane, A. Tsujimoto, W.W. Barkmeier, R. L. Erickson, M.A. Latta, M. Miyazaki, SEM observation of novel characteristic of

the dentin bond interfaces of universal adhesives, Dent. Mater. 35 (2019) 1791–1804, https://doi.org/10.1016/j.dental.2019.10.006.
[77] M. Inokoshi, K. Yoshihara, N. Nagaoka, M. Nakanishi, J. De Munck, S. Minakuchi, K. Vanmeensel, F. Zhang, Y. Yoshida, J. Vleugels, I. Naert, B. Van Meerbeek, Structural and chemical analysis of the Zirconia–Veneering ceramic interface, J. Dent. Res. 95 (2016) 102–109, https://doi.org/10.1177/0022034515608825.
[78] N. Erdman, R. Campbell, S. Asahina, Precise SEM cross section polishing via argon beam milling, Micros. Today. 14 (2006) 22–25, https://doi.org/10.1017/S155192950005762X.
[79] J.S. Park, Y.-J. Kang, S.E. Choi, Y.N. Jo, TEM sample preparation of microsized LiMn2O4 powder using an ion slicer, Appl. Microsc. 51 (2021) 19, https://doi.org/10.1186/s42649-021-00068-5.
[80] H.T. Hung, P.T. Lee, C.H. Tsai, C.R. Kao, Artifact-free microstructures of the cu–in reaction by using cryogenic broad argon beam ion polishing, J. Mater. Res. Technol. 9 (2020) 12946–12954, https://doi.org/10.1016/j.jmrt.2020.09.045.
[81] A. Gholinia, M.E. Curd, E. Bousser, K. Taylor, T. Hosman, S. Coyle, M.H. Shearer, J. Hunt, P.J. Withers, Coupled Broad Ion Beam–Scanning Electron Microscopy (BIB–SEM) for polishing and three dimensional (3D) serial section tomography (SST), Ultramicroscopy. 214 (2020) 112989, https://doi.org/10.1016/j.ultramic.2020.112989.
[82] J.T.L. Thong, K.W. Lee, W.K. Wong, Reduction of charging effects using vector scanning in the scanning electron microscope, Scanning. 23 (2001) 395–402, https://doi.org/10.1002/sca.4950230606.
[83] N.T.H. Farr, G.M. Hughes, C. Rodenburg, Monitoring carbon in Electron and ion beam deposition within FIB-SEM, Materials (Basel). 14 (2021) 3034, https://doi.org/10.3390/ma14113034.
[84] S. Hettler, M. Dries, P. Hermann, M. Obermair, D. Gerthsen, M. Malac, Carbon contamination in scanning transmission electron microscopy and its impact on phase-plate applications, Micron. 96 (2017) 38–47, https://doi.org/10.1016/j.micron.2017.02.002.
[85] C. Fager, M. Röding, A. Olsson, N. Lorén, C. von Corswant, A. Särkkä, E. Olsson, Optimization of FIB–SEM tomography and reconstruction for soft, porous, and poorly conducting materials, Microsc. Microanal. (2020) 1–9, https://doi.org/10.1017/S1431927620001592.
[86] E. Knapek, J. Dubochet, Beam damage to organic material is considerably reduced in cryo-electron microscopy, J. Mol. Biol. 141 (1980) 147–161, https://doi.org/10.1016/0022-2836(80)90382-4.
[87] K. Rykaczewski, D.G. Mieritz, M. Liu, Y. Ma, E.B. Iezzi, X. Sun, L.P. Wang, K. N. Solanki, D.-K. Seo, R.Y. Wang, FAR-reaching geometrical artefacts due to thermal decomposition of polymeric coatings around focused ion beam milled pigment particles: FAR REACHING FIB INDUCED ARTEFACTS, J. Microsc. 262 (2016) 316–325, https://doi.org/10.1111/jmi.12367.
[88] D. Drobne, M. Milani, V. Lešer, F. Tatti, Surface damage induced by FIB milling and imaging of biological samples is controllable, Microsc. Res. Tech. 70 (2007) 895–903, https://doi.org/10.1002/jemt.20494.
[89] R.D. Kelley, K. Song, B.V. Leer, D. Wall, L. Kwakman, Xe+ FIB milling and measurement of amorphous silicon damage, Microsc. Microanal. 19 (2013) 862–863, https://doi.org/10.1017/S1431927613006302.
[90] S. Liu, L. Sun, J. Gao, K. Li, A fast curtain-removal method for 3D FIB-SEM images of heterogeneous minerals, J. Microsc. 272 (2018) 3–11, https://doi.org/10.1111/jmi.12723.
[91] Y. Xiao, J. Wehrs, H. Ma, T. Al-Samman, S. Korte-Kerzel, M. Göken, J. Michler, R. Spolenak, J.M. Wheeler, Investigation of the deformation behavior of aluminum micropillars produced by focused ion beam machining using Ga and Xe ions, Scr. Mater. 127 (2017) 191–194, https://doi.org/10.1016/j.scriptamat.2016.08.028.
[92] J.R. Michael, L.A. Giannuzzi, M.G. Burke, X.L. Zhong, Mechanism of FIB-induced phase transformation in austenitic steel, Microsc. Microanal. (2021) 1–13, https://doi.org/10.1017/S1431927621013738.
[93] T. Vermeij, E. Plancher, C.C. Tasan, Preventing damage and redeposition during focused ion beam milling: the "umbrella" method, Ultramicroscopy. 186 (2018) 35–41, https://doi.org/10.1016/j.ultramic.2017.12.012.
[94] S.N. Bhavsar, S. Aravindan, P.V. Rao, Experimental investigation of redeposition during focused ion beam milling of high speed steel, Precis. Eng. 36 (2012) 408–413, https://doi.org/10.1016/j.precisioneng.2011.12.005.
[95] D.A.M. de Winter, J.J.L. Mulders, Redeposition characteristics of focused ion beam milling for nanofabrication, J. Vac. Sci. Technol. B 25 (2007) 2215, https://doi.org/10.1116/1.2806973.
[96] J. Reuteler, FIB Artifacts and How to Overcome Them, EuFN FIB Workshop, Graz, July 4th/5th, 2017. (n.d.) 25.
[97] D.J. Stokes, M.F. Hayles, in: M.T. Postek, D.E. Newbury, S.F. Platek, D.C. Joy (Eds.), Methodologies for the Preparation of Soft Materials Using cryoFIB SEM, 2009, p. 73780G, https://doi.org/10.1117/12.821834. Monterey, CA.
[98] A. Wolff, N. Klingner, W. Thompson, Y. Zhou, J. Lin, Y.Y. Peng, J.A.M. Ramshaw, Y. Xiao, Modelling of focused ion beam induced increases in sample temperature: a case study of heat damage in biological samples: MODELLING OF FOCUSED ION BEAM INDUCED INCREASES IN SAMPLE TEMPERATURE, J. Microsc. 272 (2018) 47–59, https://doi.org/10.1111/jmi.12731.
[99] S. Kim, M. Jeong Park, N.P. Balsara, G. Liu, A.M. Minor, Minimization of focused ion beam damage in nanostructured polymer thin films, Ultramicroscopy. 111 (2011) 191–199, https://doi.org/10.1016/j.ultramic.2010.11.027.
[100] Y. Katayanagi, T. Shimizu, Y. Hashimasa, N. Matsushita, Y. Yamazaki, T. Yamaguchi, Cross-sectional observation of nanostructured catalyst layer of polymer electrolyte fuel cell using FIB/SEM, J. Power Sources 280 (2015) 210–216, https://doi.org/10.1016/j.jpowsour.2015.01.085.
[101] C.A. Ventura, C. Cannavà, R. Stancanelli, D. Paolino, D. Cosco, A. La Mantia, R. Pignatello, S. Tommasini, Gemcitabine-loaded chitosan microspheres. Characterization and biological in vitro evaluation, Biomed. Microdevices 13 (2011) 799–807, https://doi.org/10.1007/s10544-011-9550-6.
[102] M. Agnoletti, C. Rodríguez-Rodríguez, S.N. Kłodzińska, T.V.F. Esposito, K. Saatchi, H. Mørck Nielsen, U.O. Häfeli, Monosized polymeric microspheres designed for passive lung targeting: biodistribution and pharmacokinetics after intravenous administration, ACS Nano (2020), https://doi.org/10.1021/acsnano.9b09773.
[103] F. Wan, M.J. Maltesen, S.K. Andersen, S. Bjerregaard, C. Foged, J. Rantanen, M. Yang, One-step production of protein-loaded PLGA microparticles via spray drying using 3-fluid nozzle, Pharm. Res. 31 (2014) 1967–1977, https://doi.org/10.1007/s11095-014-1299-1.
[104] A.G. Clark, R. Wang, J. Lomeo, Y. Wang, A. Zhu, M. Shen, Q. Bao, D.J. Burgess, B. Qin, S. Zhang, Investigating structural attributes of drug encapsulated microspheres with quantitative X-ray imaging, J. Control. Release 358 (2023) 626–635, https://doi.org/10.1016/j.jconrel.2023.05.019.
[105] Tomoiaga, Alina Maria, Ochiuz, Lacramioara, Vasile, Aurelia, Sonochemical Development of Magnetic Nanoporous Therapeutic Systems as Carriers for 5-Fluorouracil (JNDT v1n1a4), Savvy Publishers. (n.d.). http://savvysciencepublisher.com/downloads/jndtv1n1a4/ (accessed May 6, 2021).
[106] I. Mylonaki, E. Allémann, F. Delie, O. Jordan, Imaging the porous structure in the core of degrading PLGA microparticles: the effect of molecular weight, J. Control. Release 286 (2018) 231–239, https://doi.org/10.1016/j.jconrel.2018.07.044.
[107] A.K. Schomberg, A. Diener, I. Wünsch, J.H. Finke, A. Kwade, The use of X-ray microtomography to investigate the microstructure of pharmaceutical tablets: potentials and comparison to common physical methods, Intern. J. Pharm.: X. 3 (2021) 100090, https://doi.org/10.1016/j.ijpx.2021.100090.
[108] T. Yamamura, T. Ohta, T. Taira, Y. Ogawa, Y. Sakai, K. Moribe, K. Yamamoto, Effects of automated external lubrication on tablet properties and the stability of eprazinone hydrochloride, Int. J. Pharm. 370 (2009) 1–7, https://doi.org/10.1016/j.ijpharm.2008.11.007.
[109] F. Lecomte, J. Siepmann, M. Walther, R.J. MacRae, R. Bodmeier, Blends of enteric and GIT-insoluble polymers used for film coating: physicochemical characterization and drug release patterns, J. Control. Release 89 (2003) 457–471, https://doi.org/10.1016/S0168-3659(03)00155-X.
[110] M.A. Frohoff-HuËlsmann, B.C. Lippold, J.W. McGinity, Aqueous ethyl cellulose dispersion containing plasticizers of different water solubility and hydroxypropyl methyl-cellulose as coating material for diffusion pellets II: properties of sprayed ®lmsq, Eur. J. Pharm. Biopharm. 9 (1999).
[111] H. Häbel, H. Andersson, A. Olsson, E. Olsson, A. Larsson, A. Särkkä, Characterization of pore structure of polymer blended films used for controlled drug release, J. Control. Release 222 (2016) 151–158, https://doi.org/10.1016/j.jconrel.2015.12.011.
[112] H. Andersson, H. Häbel, A. Olsson, S. Sandhagen, C. von Corswant, J. Hjärtstam, M. Persson, M. Stading, A. Larsson, The influence of the molecular weight of the water-soluble polymer on phase-separated films for controlled release, Int. J. Pharm. 511 (2016) 223–235, https://doi.org/10.1016/j.ijpharm.2016.06.058.
[113] M. Marucci, J. Hjärtstam, G. Ragnarsson, F. Iselau, A. Axelsson, Coated formulations: new insights into the release mechanism and changes in the film properties with a novel release cell, J. Control. Release 136 (2009) 206–212, https://doi.org/10.1016/j.jconrel.2009.02.017.
[114] F. Skärberg, C. Fager, F. Mendoza-Lara, M. Josefson, E. Olsson, N. Lorén, M. Röding, Convolutional neural networks for segmentation of FIB-SEM nanotomography data from porous polymer films for controlled drug release, J. Microsc. 283 (2021) 51–63, https://doi.org/10.1111/jmi.13007.
[115] M. Röding, C. Fager, A. Olsson, C. von Corswant, E. Olsson, N. Lorén, Three-dimensional reconstruction of porous polymer films from FIB-SEM nanotomography data using random forests, J. Microsc. 281 (2021) 76–86, https://doi.org/10.1111/jmi.12950.
[116] S. Barman, C. Fager, M. Röding, N. Lorén, C. von Corswant, E. Olsson, D. Bolin, H. Rootzén, New characterization measures of pore shape and connectivity applied to coatings used for controlled drug release, JPharmSci. 0 (2021), https://doi.org/10.1016/j.xphs.2021.02.024.
[117] C. Fager, S. Barman, M. Röding, A. Olsson, N. Lorén, C. von Corswant, D. Bolin, H. Rootzén, E. Olsson, 3D high spatial resolution visualisation and quantification of interconnectivity in polymer films, Int. J. Pharm. 587 (2020) 119622, https://doi.org/10.1016/j.ijpharm.2020.119622.
[118] C. Fager, T. Gebäck, J. Hjärtstam, M. Röding, A. Olsson, N. Lorén, C. von Corswant, A. Särkkä, E. Olsson, Correlating 3D porous structure in polymer films with mass transport properties using FIB-SEM tomography, Chem. Eng. Sci. X (2021) 100109, https://doi.org/10.1016/j.cesx.2021.100109.
[119] S. Zhang, G. Byrne, Characterization of transport mechanisms for controlled release polymer membranes using focused ion beam scanning electron microscopy image-based modelling, J. Drug Deliv. Sci. Technol. 61 (2021) 102136, https://doi.org/10.1016/j.jddst.2020.102136.
[120] C.E. Pyo, M. Song, J.H. Chang, Preparation and in vitro cytotoxicity assessments of spherical silica-encapsulated liposome particles for highly efficient drug carriers, ACS Appl. Bio Mater. 4 (2021) 1350–1359, https://doi.org/10.1021/acsabm.0c01240.
[121] J. Radtke, R. Wiedey, P. Kleinebudde, Alternatives to titanium dioxide in tablet coating, Pharm. Dev. Technol. 26 (2021) 989–999, https://doi.org/10.1080/10837450.2021.1968900.
[122] J.-C. Lin, W. Heeschen, J. Reffner, J. Hook, Three-dimensional characterization of pigment dispersion in dried paint films using focused ion beam–scanning electron

microscopy, Microsc. Microanal. 18 (2012) 266–271, https://doi.org/10.1017/S143192761101244X.
[123] M. Goslinska, I. Selmer, C. Kleemann, U. Kulozik, I. Smirnova, S. Heinrich, Novel technique for measurement of coating layer thickness of fine and porous particles using focused ion beam, Particuology. 42 (2019) 190–198, https://doi.org/10.1016/j.partic.2018.03.002.
[124] J.W. Jung, S.H. Han, S.Ah. Kim, E.K. Kim, K.Y. Seo, T. Kim, Evaluation of pigment location in tinted soft contact lenses, Contact Lens Anterior Eye. 39 (2016) 210–216, https://doi.org/10.1016/j.clae.2016.01.008.
[125] K. Gou, Y. Wang, X. Guo, Y. Wang, Y. Bian, H. Zhao, Y. Guo, Y. Pang, L. Xie, S. Li, H. Li, Carboxyl-Functionalized Mesoporous Silica Nanoparticles for the Controlled Delivery of Poorly Water-soluble Non-steroidal Anti-inflammatory Drugs, (n.d.) 17.
[126] S.G. Gumaste, S.A. Pawlak, D.M. Dalrymple, C.J. Nider, L.D. Trombetta, A.T. M. Serajuddin, Development of solid SEDDS, IV: effect of adsorbed lipid and surfactant on tableting properties and surface structures of different silicates, Pharm. Res. 30 (2013) 3170–3185, https://doi.org/10.1007/s11095-013-1114-4.
[127] H. Takeuchi, S. Nagira, H. Yamamoto, Y. Kawashima, Solid dispersion particles of amorphous indomethacin with fine porous silica particles by using spray-drying method, Int. J. Pharm. 293 (2005) 155–164, https://doi.org/10.1016/j.ijpharm.2004.12.019.
[128] H. Takeuchi, S. Nagira, S. Tanimura, H. Yamamoto, Y. Kawashima, Tabletting of solid dispersion particles consisting of indomethacin and porous silica particles, Chem. Pharm. Bull. 53 (2005) 487–491, https://doi.org/10.1248/cpb.53.487.
[129] M. Farzan, R. Roth, G. Québatte, J. Schoelkopf, J. Huwyler, M. Puchkov, Loading of porous functionalized calcium carbonate microparticles: distribution analysis with focused ion beam Electron microscopy and mercury Porosimetry, Pharmaceutics. 11 (2019) 32, https://doi.org/10.3390/pharmaceutics11010032.
[130] T. Stirnimann, S. Atria, J. Schoelkopf, P.A.C. Gane, R. Alles, J. Huwyler, M. Puchkov, Compaction of functionalized calcium carbonate, a porous and crystalline microparticulate material with a lamellar surface, Int. J. Pharm. 466 (2014) 266–275, https://doi.org/10.1016/j.ijpharm.2014.03.027.
[131] M. Farzan, G. Québatte, K. Strittmatter, F.M. Hilty, J. Schoelkopf, J. Huwyler, M. Puchkov, Spontaneous in situ formation of liposomes from inert porous microparticles for Oral drug delivery, Pharmaceutics. 12 (2020) 777, https://doi.org/10.3390/pharmaceutics12080777.
[132] P. Zhang, J. Forsgren, M. Strømme, Stabilisation of amorphous ibuprofen in Upsalite, a mesoporous magnesium carbonate, as an approach to increasing the aqueous solubility of poorly soluble drugs, Int. J. Pharm. 472 (2014) 185–191, https://doi.org/10.1016/j.ijpharm.2014.06.025.
[133] C. Alvebratt, T.J. Dening, M. Åhlén, O. Cheung, M. Strømme, A. Gogoll, C. A. Prestidge, C.A.S. Bergström, In vitro performance and chemical stability of lipid-based formulations encapsulated in a mesoporous magnesium carbonate carrier, Pharmaceutics. 12 (2020) E426, https://doi.org/10.3390/pharmaceutics12050426.
[134] H. Giesche, Mercury Porosimetry: a general (practical) overview, Part. Part. Syst. Charact. 23 (2006) 9–19, https://doi.org/10.1002/ppsc.200601009.
[135] G.P. Johnston, D.M. Smith, I. Melendez, A.J. Hurd, Compression effects in mercury porosimetry, Powder Technol. 61 (1990) 289–294, https://doi.org/10.1016/0032-5910(90)80093-E.
[136] A. Endo, M. Yamada, S. Kataoka, T. Sano, Y. Inagi, A. Miyaki, Direct observation of surface structure of mesoporous silica with low acceleration voltage FE-SEM, Colloids Surf. A Physicochem. Eng. Asp. 357 (2010) 11–16, https://doi.org/10.1016/j.colsurfa.2009.11.026.
[137] R. Vehring, Pharmaceutical particle engineering via spray drying, Pharm. Res. 25 (2008) 999–1022, https://doi.org/10.1007/s11095-007-9475-1.
[138] D. Heng, P. Tang, J.M. Cairney, H.-K. Chan, D.J. Cutler, R. Salama, J. Yun, Focused-ion-beam milling: a novel approach to probing the interior of particles used for inhalation aerosols, Pharm. Res. 24 (2007) 1608–1617, https://doi.org/10.1007/s11095-007-9276-6.
[139] H. Xi, A. Zhu, G.R. Klinzing, L. Zhou, S. Zhang, A.J. Gmitter, K. Ploeger, P. Sundararajan, M. Mahjour, W. Xu, Characterization of spray dried particles through microstructural imaging, J. Pharm. Sci. (2020), https://doi.org/10.1016/j.xphs.2020.07.032.
[140] S. Poozesh, N. Setiawan, F. Arce, P. Sundararajan, J.D. Rocca, A. Rumondor, D. Wei, R. Wenslow, H. Xi, S. Zhang, J. Stellabott, Y. Su, J. Moser, P.J. Marsac, Understanding the process-product-performance interplay of spray dried drug-polymer systems through complete structural and chemical characterization of single spray dried particles, Powder Technol. 320 (2017) 685–695, https://doi.org/10.1016/j.powtec.2017.07.042.
[141] J.A. Bouwstra, R.W.J. Helder, A. El Ghalbzouri, Human skin equivalents: impaired barrier function in relation to the lipid and protein properties of the stratum corneum, Adv. Drug Deliv. Rev. 175 (2021) 113802, https://doi.org/10.1016/j.addr.2021.05.012.
[142] A.S. Hanafy, D. Dietrich, G. Fricker, A. Lamprecht, Blood-brain barrier models: rationale for selection, Adv. Drug Deliv. Rev. 176 (2021) 113859, https://doi.org/10.1016/j.addr.2021.113859.
[143] J.P. Schneider, C. Wrede, C. Mühlfeld, The three-dimensional ultrastructure of the human alveolar epithelium revealed by focused ion beam Electron microscopy, Int. J. Mol. Sci. 21 (2020) 1089, https://doi.org/10.3390/ijms21031089.
[144] Y. Kawasaki, Y. Hosoyamada, T. Miyaki, J. Yamaguchi, S. Kakuta, T. Sakai, K. Ichimura, Three-dimensional architecture of glomerular endothelial cells revealed by FIB-SEM tomography, Front. Cell Develop. Biol. 9 (2021) 339, https://doi.org/10.3389/fcell.2021.653472.
[145] L. Hollander, H. Han, M. Winter, L. Svensson, S. Masich, B. Daneholt, L. Norlén, Skin lamellar bodies are not discrete vesicles but part of a Tubuloreticular network, Acta. Derm. Venerol. 96 (2016) 303–308, https://doi.org/10.2340/00015555-2249.
[146] E. Lindberg, Y. Baumer, E.S. Stempinski, J.A. Rodante, T.M. Powell-Wiley, A. K. Dey, S. Nakajima, M.P. Playford, C.K.E. Bleck, N.N. Mehta, Nanotomography of lesional skin using electron microscopy reveals cytosolic release of nuclear DNA in psoriasis, JAAD Case Reports. 9 (2021) 9–14, https://doi.org/10.1016/j.jdcr.2020.12.024.
[147] J.C. Tapia, N. Kasthuri, K.J. Hayworth, R. Schalek, J.W. Lichtman, S.J. Smith, J. Buchanan, High-contrast en bloc staining of neuronal tissue for field emission scanning electron microscopy, Nat. Protoc. 7 (2012) 193–206, https://doi.org/10.1038/nprot.2011.439.
[148] A. Takahashi-Nakazato, L.K. Parajuli, H. Iwasaki, S. Tanaka, S. Okabe, Ultrastructural observation of glutamatergic synapses by focused ion beam scanning Electron microscopy (FIB/SEM), Methods Mol. Biol. 2019 (1941) 17–27, https://doi.org/10.1007/978-1-4939-9077-1_2.
[149] A.J. Bushby, K.M.Y. P'ng, R.D. Young, C. Pinali, C. Knupp, A.J. Quantock, Imaging three-dimensional tissue architectures by focused ion beam scanning electron microscopy, Nat. Protoc. 6 (2011) 845–858, https://doi.org/10.1038/nprot.2011.332.
[150] K. Murata, A. Hirata, K. Ohta, H. Enaida, K. Nakamura, Morphometric analysis in mouse scleral fibroblasts using focused ion beam/scanning electron microscopy, Sci. Rep. 9 (2019) 6329, https://doi.org/10.1038/s41598-019-42758-x.
[151] S. Kappes, T. Faber, L. Nelleßen, T. Yesilkaya, U. Bock, A. Lamprecht, Improving Transungual permeation study design by increased bovine hoof membrane thickness and subsequent infection, Pharmaceutics. 13 (2021) 2098, https://doi.org/10.3390/pharmaceutics13122098.
[152] T. Ellis, M. Chiappi, A. García-Trenco, M. Al-Ejji, S. Sarkar, T.K. Georgiou, M.S. P. Shaffer, T.D. Tetley, S. Schwander, M.P. Ryan, A.E. Porter, Multimetallic microparticles increase the potency of rifampicin against intracellular mycobacterium tuberculosis, ACS Nano 12 (2018) 5228–5240, https://doi.org/10.1021/acsnano.7b08264.
[153] H. Klingberg, L.B. Oddershede, K. Loeschner, E.H. Larsen, S. Loft, P. Møller, Uptake of gold nanoparticles in primary human endothelial cells, Toxicol. Res. 4 (2015) 655–666, https://doi.org/10.1039/C4TX00061G.
[154] E. Guehrs, M. Schneider, C.M. Günther, P. Hessing, K. Heitz, D. Wittke, A. López-Serrano Oliver, N. Jakubowski, J. Plendl, S. Eisebitt, A. Haase, Quantification of silver nanoparticle uptake and distribution within individual human macrophages by FIB/SEM slice and view, J. Nanobiotechnol. 15 (2017), https://doi.org/10.1186/s12951-017-0255-8.
[155] H. Margus, K. Padari, M. Pooga, Insights into cell entry and intracellular trafficking of peptide and protein drugs provided by electron microscopy, Adv. Drug Deliv. Rev. 65 (2013) 1031–1038, https://doi.org/10.1016/j.addr.2013.04.013.
[156] C. Brandenberger, C. Mühlfeld, Z. Ali, A.-G. Lenz, O. Schmid, W.J. Parak, P. Gehr, B. Rothen-Rutishauser, Quantitative evaluation of cellular uptake and trafficking of plain and polyethylene glycol-coated gold nanoparticles, Small. 6 (2010) 1669–1678, https://doi.org/10.1002/smll.201000528.
[157] V. Mollo, P. Scognamiglio, A. Marino, G. Ciofani, F. Santoro, Probing the ultrastructure of spheroids and their uptake of magnetic nanoparticles by FIB–SEM, Adv. Mater. Technol. 5 (2020) 1900687, https://doi.org/10.1002/admt.201900687.
[158] M.P. Calatayud, B. Sanz, V. Raffa, C. Riggio, M.R. Ibarra, G.F. Goya, The effect of surface charge of functionalized Fe3O4 nanoparticles on protein adsorption and cell uptake, Biomaterials. 35 (2014) 6389–6399, https://doi.org/10.1016/j.biomaterials.2014.04.009.
[159] X. He, Z. Yuan, W. Kao, D. Miller, S.K. Li, Y.C. Park, Size-exclusive Nanoporous biodegradable PLGA capsules for drug delivery implants and in vivo stability in the posterior segment, ACS Appl. Bio Mater. 3 (2020) 1722–1729, https://doi.org/10.1021/acsabm.0c00027.
[160] U. Stachewicz, T. Qiao, S.C.F. Rawlinson, F.V. Almeida, W.-Q. Li, M. Cattell, A. H. Barber, 3D imaging of cell interactions with electrospun PLGA nanofiber membranes for bone regeneration, Acta Biomater. 27 (2015) 88–100, https://doi.org/10.1016/j.actbio.2015.09.003.
[161] Y. Chen, S. Aslanoglou, T. Murayama, G. Gervinskas, L.I. Fitzgerald, S. Sriram, J. Tian, A.P.R. Johnston, Y. Morikawa, K. Suu, R. Elnathan, N.H. Voelcker, Silicon-nanotube-mediated intracellular delivery enables ex vivo gene editing, Adv. Mater. 32 (2020) 2000036, https://doi.org/10.1002/adma.202000036.
[162] A. Friedmann, A. Cismak, C. Tautorat, P.J. Koester, W. Baumann, J. Held, J. Gaspar, P. Ruther, O. Paul, A. Heilmann, FIB preparation and SEM investigations for three-dimensional analysis of cell cultures on microneedle arrays, Scanning. 34 (2012) 221–229, https://doi.org/10.1002/sca.20297.
[163] R. Wierzbicki, C. Købler, M.R.B. Jensen, J. Łopacińska, M.S. Schmidt, M. Skolimowski, F. Abeille, K. Qvortrup, K. Mølhave, Mapping the complex morphology of cell interactions with nanowire substrates using FIB-SEM, PLoS One 8 (2013) e53307, https://doi.org/10.1371/journal.pone.0053307.
[164] N.D. Donahue, H. Acar, S. Wilhelm, Concepts of nanoparticle cellular uptake, intracellular trafficking, and kinetics in nanomedicine, Adv. Drug Deliv. Rev. 143 (2019) 68–96, https://doi.org/10.1016/j.addr.2019.04.008.
[165] P. Watson, Intracellular trafficking pathways and drug delivery: fluorescence imaging of living and fixed cells, Adv. Drug Deliv. Rev. 57 (2005) 43–61, https://doi.org/10.1016/j.addr.2004.05.003.
[166] N. Veiga, Y. Diesendruck, D. Peer, Targeted lipid nanoparticles for RNA therapeutics and immunomodulation in leukocytes, Adv. Drug Deliv. Rev. 159 (2020) 364–376, https://doi.org/10.1016/j.addr.2020.04.002.
[167] Y. Shu, F. Pi, A. Sharma, M. Rajabi, F. Haque, D. Shu, M. Leggas, B.M. Evers, P. Guo, Stable RNA nanoparticles as potential new generation drugs for cancer

therapy, Adv. Drug Deliv. Rev. 66 (2014) 74–89, https://doi.org/10.1016/j.addr.2013.11.006.
[168] M. Nishikawa, M. Tan, W. Liao, K. Kusamori, Nanostructured DNA for the delivery of therapeutic agents, Adv. Drug Deliv. Rev. 147 (2019) 29–36, https://doi.org/10.1016/j.addr.2019.09.004.
[169] B. Gupta, T. Levchenko, V. Torchilin, Intracellular delivery of large molecules and small particles by cell-penetrating proteins and peptides, Adv. Drug Deliv. Rev. 57 (2005) 637–651, https://doi.org/10.1016/j.addr.2004.10.007.
[170] M. Durán-Lobato, A.M. López-Estévez, A.S. Cordeiro, T.G. Dacoba, J. Crecente-Campo, D. Torres, M.J. Alonso, Nanotechnologies for the delivery of biologicals: historical perspective and current landscape, Adv. Drug Deliv. Rev. 176 (2021) 113899, https://doi.org/10.1016/j.addr.2021.113899.
[171] T. Andrian, P. Delcanale, S. Pujals, L. Albertazzi, Correlating super-resolution microscopy and transmission Electron microscopy reveals multiparametric heterogeneity in nanoparticles, Nano Lett. 21 (2021) 5360–5368, https://doi.org/10.1021/acs.nanolett.1c01666.
[172] Y.-C. Chuang, W.-Y. Yen, L. Zhang, W. Bahou, M. Simon, M. Rafailovich, C.-C. Chang, Using new 3D CLEM imaging technique to investigate the effects of substrate mechanics on cellular uptake of nanoparticle, Microsc. Microanal. 23 (2017) 1302–1303, https://doi.org/10.1017/S1431927617007176.
[173] J. Fokkema, J. Fermie, N. Liv, D.J. van den Heuvel, T.O.M. Konings, G.A. Blab, A. Meijerink, J. Klumperman, H.C. Gerritsen, Fluorescently labelled silica coated gold nanoparticles as fiducial markers for correlative light and Electron microscopy, Sci. Rep. 8 (2018) 13625, https://doi.org/10.1038/s41598-018-31836-1.
[174] M. Jung, T.K. Kim, H.-N. Woo, J.Y. Mun, H. Lee, C.-G. Pack, Correlative light and electron microscopy for nanoparticle–cell interaction and protein localization, in: J.K. Kim, J.K. Kim, C.-G. Pack (Eds.), Advanced Imaging and Bio Techniques for Convergence Science, Springer, Singapore, 2021, pp. 115–132, https://doi.org/10.1007/978-981-33-6064-8_6.
[175] N. de Souza, Super-resolution CLEM, Nat. Methods 12 (2015) 37, https://doi.org/10.1038/nmeth.3239.
[176] FY 2020 GDUFA Science and Research Report, 2020, p. 138.
[177] A.A. Wanner, M.A. Kirschmann, C. Genoud, Challenges of microtome-based serial block-face scanning electron microscopy in neuroscience, J. Microsc. 259 (2015) 137–142, https://doi.org/10.1111/jmi.12244.
[178] K.L. Briggman, D.D. Bock, Volume electron microscopy for neuronal circuit reconstruction, Curr. Opin. Neurobiol. 22 (2012) 154–161, https://doi.org/10.1016/j.conb.2011.10.022.
[179] L. Heinrich, D. Bennett, D. Ackerman, W. Park, J. Bogovic, N. Eckstein, A. Petruncio, J. Clements, S. Pang, C.S. Xu, J. Funke, W. Korff, H.F. Hess, J. Lippincott-Schwartz, S. Saalfeld, A.V. Weigel, Whole-cell organelle segmentation in volume electron microscopy, Nature. 599 (2021) 141–146, https://doi.org/10.1038/s41586-021-03977-3.
[180] M. Malatesta, Transmission Electron microscopy as a powerful tool to investigate the interaction of nanoparticles with subcellular structures, Int. J. Mol. Sci. 22 (2021) 12789, https://doi.org/10.3390/ijms222312789.
[181] D.J. Klionsky, et al., Guidelines for the use and interpretation of assays for monitoring autophagy (4th edition)1, Autophagy. 17 (2021) 1–382, https://doi.org/10.1080/15548627.2020.1797280.
[182] A. Nakashima, K. Higashisaka, T. Kusabiraki, A. Aoki, A. Ushijima, Y. Ono, S. Tsuda, T. Shima, O. Yoshino, K. Nagano, Y. Yoshioka, Y. Tsutsumi, S. Saito, Autophagy is a new protective mechanism against the cytotoxicity of platinum nanoparticles in human trophoblasts, Sci. Rep. 9 (2019) 5478, https://doi.org/10.1038/s41598-019-41927-2.
[183] L. Guo, N. He, Y. Zhao, T. Liu, Y. Deng, Autophagy modulated by inorganic nanomaterials, Theranostics. 10 (2020) 3206–3222, https://doi.org/10.7150/thno.40414.
[184] X. Feng, Y. Zhang, C. Zhang, X. Lai, Y. Zhang, J. Wu, C. Hu, L. Shao, Nanomaterial-mediated autophagy: coexisting hazard and health benefits in biomedicine, Part. Fibre Toxicol. 17 (2020) 53, https://doi.org/10.1186/s12989-020-00372-0.
[185] R.-J. Chen, Y.-Y. Chen, M.-Y. Liao, Y.-H. Lee, Z.-Y. Chen, S.-J. Yan, Y.-L. Yeh, L.-X. Yang, Y.-L. Lee, Y.-H. Wu, Y.-J. Wang, The current understanding of autophagy in nanomaterial toxicity and its implementation in safety assessment-related alternative testing strategies, Int. J. Mol. Sci. 21 (2020) 2387, https://doi.org/10.3390/ijms21072387.
[186] N. Mizushima, T. Yoshimori, B. Levine, Methods in mammalian autophagy research, Cell. 140 (2010) 313–326, https://doi.org/10.1016/j.cell.2010.01.028.
[187] G. Wang, Y. Tan, H. Wang, P. Zhou, Autophagy promotes degradation of polyethyleneimine–alginate nanoparticles in endothelial progenitor cells, Int. J. Nanomedicine 12 (2017) 6661–6675, https://doi.org/10.2147/IJN.S141592.
[188] J. Gilleron, W. Querbes, A. Zeigerer, A. Borodovsky, G. Marsico, U. Schubert, K. Manygoats, S. Seifert, C. Andree, M. Stöter, H. Epstein-Barash, L. Zhang, V. Koteliansky, K. Fitzgerald, E. Fava, M. Bickle, Y. Kalaidzidis, A. Akinc, M. Maier, M. Zerial, Image-based analysis of lipid nanoparticle–mediated siRNA delivery, intracellular trafficking and endosomal escape, Nat. Biotechnol. 31 (2013) 638–646, https://doi.org/10.1038/nbt.2612.
[189] D.M. Jorgens, J.L. Inman, M. Wojcik, C. Robertson, H. Palsdottir, W.-T. Tsai, H. Huang, A. Bruni-Cardoso, C.S. López, M.J. Bissell, K. Xu, M. Auer, Deep nuclear invaginations are linked to cytoskeletal filaments – integrated bioimaging of epithelial cells in 3D culture, J. Cell Sci. 130 (2017) 177–189, https://doi.org/10.1242/jcs.190967.
[190] M. Wittmann, G. Queisser, A. Eder, J.S. Wiegert, C.P. Bengtson, A. Hellwig, G. Wittum, H. Bading, Synaptic activity induces dramatic changes in the geometry of the cell nucleus: interplay between nuclear structure, histone H3 phosphorylation, and nuclear calcium signaling, J. Neurosci. 29 (2009) 14687–14700, https://doi.org/10.1523/JNEUROSCI.1160-09.2009.
[191] P. De Magistris, W. Antonin, The dynamic nature of the nuclear envelope, Curr. Biol. 28 (2018) R487–R497, https://doi.org/10.1016/j.cub.2018.01.073.
[192] G. Ferri, G. Fiume, D. Pozzi, G. Caracciolo, F. Cardarelli, Probing the role of nuclear-envelope invaginations in the nuclear-entry route of lipofected DNA by multi-channel 3D confocal microscopy, Colloids Surf. B: Biointerfaces 205 (2021) 111881, https://doi.org/10.1016/j.colsurfb.2021.111881.
[193] V. Bello, G. Mattei, P. Mazzoldi, N. Vivenza, P. Gasco, J.M. Idee, C. Robic, E. Borsella, Transmission Electron microscopy of lipid vesicles for drug delivery: comparison between positive and negative staining, Microsc. Microanal. 16 (2010) 456–461, https://doi.org/10.1017/S1431927610093645.
[194] M. Costanzo, E. Esposito, M. Sguizzato, M.A. Lacavalla, M. Drechsler, G. Valacchi, C. Zancanaro, M. Malatesta, Formulative study and intracellular fate evaluation of ethosomes and transethosomes for vitamin D3 delivery, Int. J. Mol. Sci. 22 (2021) 5341, https://doi.org/10.3390/ijms22105341.
[195] M. Sguizzato, F. Ferrara, S.S. Hallan, A. Baldisserotto, M. Drechsler, M. Malatesta, M. Costanzo, R. Cortesi, C. Puglia, G. Valacchi, E. Esposito, Ethosomes and transethosomes for mangiferin transdermal delivery, Antioxidants. 10 (2021) 768, https://doi.org/10.3390/antiox10050768.
[196] M. Costanzo, L. Scolaro, G. Berlier, A. Marengo, S. Grecchi, C. Zancanaro, M. Malatesta, S. Arpicco, Cell uptake and intracellular fate of phospholipidic manganese-based nanoparticles, Int. J. Pharm. 508 (2016) 83–91, https://doi.org/10.1016/j.ijpharm.2016.05.019.
[197] M. Costanzo, M. Malatesta, Embedding cell monolayers to investigate nanoparticle-plasmalemma interactions at transmission electron microscopy, Eur. J. Histochem. 63 (2019) 3026, https://doi.org/10.4081/ejh.2019.3026.